Environmental Chemistry Letters (2022) 20:2929–2949
https://doi.org/10.1007/s10311-022-01469-y

REVIEW

Electrocatalytic conversion of nitrate waste into ammonia: a review

Jayaraman Theerthagiri[1] · Juhyeon Park[1] · Himadri Tanaya Das[2] · Nihila Rahamathulla[3] · Eduardo S. F. Cardoso[4] · Arun Prasad Murthy[3] · Gilberto Maia[4] · Dai-Viet N. Vo[5] · Myong Yong Choi[1]

Received: 5 May 2022 / Accepted: 27 May 2022 / Published online: 9 July 2022

Abstract

The electrocatalytic reduction of nitrate waste into ammonia allows both the removal of nitrate contaminants and an alternative production of ammonia compared to the classical Haber–Bosch industrial process. Ammonia is useful in agriculture for manufacturing fertilizers, and as a reagent in pharmaceuticals, metallurgy, explosives, and the textile industry; ammonia is also an energy carrier in the automobile industry for next-generation fuel cells. Here we review the nitrate-to-ammonia conversion by electrocatalysis of industrial and agricultural waste, with focus on catalysts, reaction intermediates, side reactions, and reaction conditions. Electron transfer is facilitated by electrocatalysts with transition metals having occupied d-orbitals with similar energy levels to that of the nitrate lowest unoccupied molecular orbital. Green electro-conversion using carbon-based materials is also discussed. Results show nitrate conversion from 53 to 99.8% and ammonia selectivity from 70 to 97.4%.

Keywords Electrochemical reduction · Electrocatalyst · Nitrate removal · Ammonia production · Selective conversion

Introduction

Nitrogen is the most abundant element in the atmosphere. Maintenance of the nitrogen cycle is as pivotal as that of the carbon cycle, as one of the biogeochemical processes that integrate the chemistry of earth and life. The ability of nitrogen to exhibit varying oxidation states ranging from + 3 to − 5 accounts for various forms, such as inert nitrogen gas, ammonia, nitrogen oxides such as NO_2 and N_2O, nitrate compounds, and ammonium compounds (Lu et al. 2021; Min et al. 2021). Among the nitrogen compounds, ammonia is one of the most important compounds. Ammonia is extensively used in manufacturing fertilizers and as a reagent in pharmaceuticals, metallurgy, refrigeration, explosives, and the textile industry, among others (Lu et al. 2021; Xiang et al. 2012). Ammonia has great potential to serve as the next-generation carbon-free energy carrier because of energy density of 22.5 MJ kg^{-1}, which is comparable with that of nonrenewable energy resources (Liu et al. 2021b; Valera-Medina et al. 2018). Compared with H_2, ammonia has a lower cost per unit of stored energy, a higher volumetric

Jayaraman Theerthagiri, Juhyeon Park, Himadri Tanaya Das, Nihila Rahamathulla, and Eduardo S. F. Cardoso contributed equally to this work.

✉ Arun Prasad Murthy
arunprasad.m@vit.ac.in

✉ Gilberto Maia
gilberto.maia@ufms.br

✉ Dai-Viet N. Vo
vndviet@ntt.edu.vn

✉ Myong Yong Choi
mychoi@gnu.ac.kr

[1] Core-Facility Center for Photochemistry & Nanomaterials, Department of Chemistry (BK21 FOUR), Research Institute of Natural Sciences, Gyeongsang National University, Jinju 52828, South Korea

[2] Centre of Excellence for Advanced Materials and Applications, Utkal University, Bhubaneswar, Odisha 751004, India

[3] Department of Chemistry, School of Advanced Sciences, Vellore Institute of Technology, Tamil Nadu, Vellore 632014, India

[4] Institute of Chemistry, Federal University of Mato Grosso Do Sul, Av. Senador Filinto Muller, 1555, Campo Grande, MS 79074–460, Brazil

[5] Center of Excellence for Green Energy and Environmental Nanomaterials (CE@GrEEN), Nguyen Tat Thanh University, 300A Nguyen Tat Thanh, District 4, Ho Chi Minh City 755414, Vietnam

energy density of 7.1–2.9 MJ L^{-1}, and a more facile production and transportation process (Valera-Medina et al. 2018). Additionally, ammonia, as a hydrogen derivative, can amend the prospective complex aspects of storing and transporting H_2 energy or can serve as an alternative energy carrier to H_2 given high gravimetric density (Fig. 1).

The versatile utilization of ammonia in various fields upscaled the global production of ammonia from 131 million metric tons in 2010 to approximately 150 million metric tons by 2021. In this context, the sustainable production of ammonia from the electrochemical reduction of nitrate can be recognized as a waste-to-wealth concept (Wang et al. 2021d). If the electrical energy required for electrochemical reduction is derived from renewable resources, this conversion process can restore the nitrogen cycle in an eco-friendly and economical manner (Min et al. 2021). The rational design and optimization of electrocatalysts with maximum efficiency and selectivity for ammonia over N_2 are still under dynamic research. As discussed below, fabricating efficient electrocatalysts for electrochemical reduction of nitrate requires a fundamental cognizance of the reaction mechanism.

Ammonia production techniques and applications

Industrial ammonia synthesis is conducted using the Haber–Bosch method (Lu et al. 2021; Shipman and Symes 2017), which involves the reaction between H_2 and N_2 at high pressure and temperature. The extreme reaction conditions necessitate high energy consumption, which is derived from fossil fuel combustion, concomitantly releasing carbon dioxide into the atmosphere (Li et al. 2021a). Statistics show that the Haber–Bosch synthesis of ammonia accounts for 11% of global carbon dioxide emissions (Hasan et al. 2021).

The anthropogenic emission of nitrate from industrial wastewater effluents can seriously pollute water resources, leading to algal blooms and anoxic conditions for aquatic flora and fauna (Morin-Crini et al. 2022; Wang et al. 2020a; Xu et al. 2019). Additionally, the accumulation of nitrates in the air and aquatic and terrestrial environments is a serious threat to human health, the balance of the ecosystem, and a quality-rich atmosphere (Liu et al. 2021a). Furthermore, the contamination of groundwater primarily with a high concentration of nitrates (NO_3^-), as well as the ingestion of these nitrates through drinking water, can lead to methemoglobinemia, increased heart rate, and nausea in humans and an increased possibility of blue baby syndrome (Barrera and Bala Chandran 2021; Prashantha Kumar et al. 2018; Velusamy et al. 2021). The dissolution of NO_3^- in water droplets in the atmosphere and the subsequent emission of nitrogen oxides can cause acid rain. The increasing rates of ammonia production, overfertilization, eutrophication, bioaccumulation of nitrogenous pollutants in the food chain, and nitrate pollutant emission into the biosphere compared with the natural balance maintained by the microorganisms in the nitrogen cycle have induced the deterioration of the nitrogen cycle.

Conventional biological denitrification as a remedy is ineffective, as requires energy inputs up to 45 MJ kgN^{-1} (Barrera and Bala Chandran 2021) and results in sludge with a high concentration of pathogenic bacteria. Physical wastewater treatment processes, such as reverse osmosis, ion exchange, and electrodialysis, are also not feasible, as

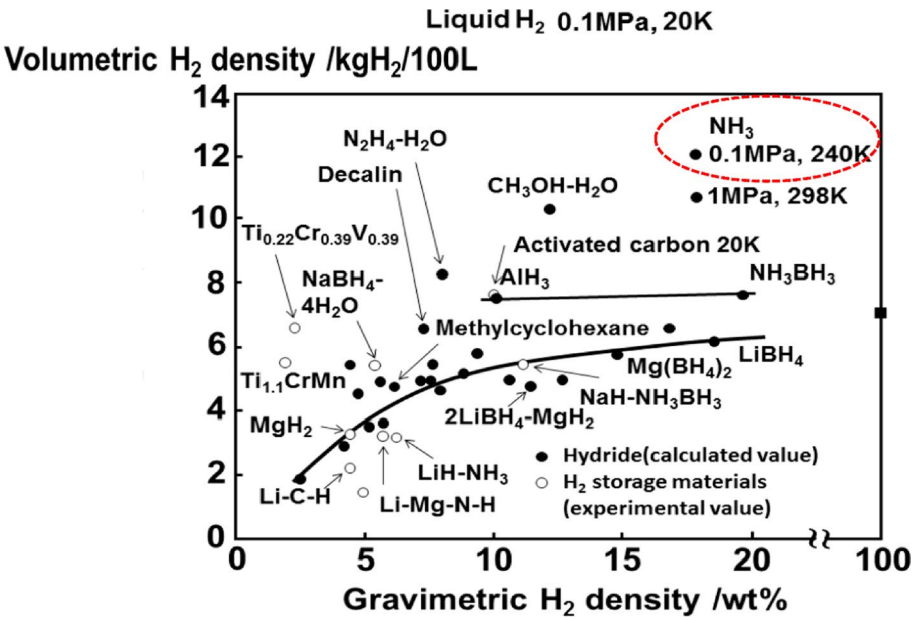

Fig. 1 Density of H_2 in H_2-carriers (packing efficiency in solids: 50%). As noticed, ammonia has the high volumetric and gravimetric densities which provides an added advantage for ammonia to be used as alternative storage of sustainable energy since H_2 facing issues on the storage and distribution. By transforming nitrate as targeted waste into value-added product of ammonia as efficient energy carrier that can be liquefied under controlled pressure, renewable energy can be delighted from positions where sustainable energy is excessive or cheap. Reproduced from reference (Hasan et al. 2021) with permission from MDPI

they produce secondary brine effluents, which should be further subjected to other treatment methods (Barrera and Bala Chandran 2021; Madhura et al. 2019; Martínez et al. 2017; Mudhoo et al. 2020). There is an increasing demand to develop wastewater treatment technologies combined with renewable energy for the constructive conversion of nitrogen contaminants to value-added products, such as ammonia (Wang et al. 2021i). Another imminent method is when chemical energy is driven by thermal, photoelectrochemical, or electric energy. Electrochemical reduction is a promising remedial approach to decreasing nitrogen-containing pollutants (Wang et al. 2021c). This method involves reducing nitrate-containing wastewater effluents to harmless dinitrogen gas or value-added ammonia (Fig. 2) (Wang et al. 2021d). The electrocatalytic conversion of nitrate-containing wastewater effluents to ammonia can be conducted under ambient temperature and pressure and can serve as an alternative remedial scientific approach to the environmentally unfriendly Haber–Bosch synthesis of ammonia (Lu et al. 2021).

Experimental aspects of electrocatalytic reduction of nitrates

The electrolysis of nitrates can be conducted through potentiostatic or galvanostatic methods. The potentiostatic method involves providing a constant fixed electric potential from an external source, whereas the galvanostatic method involves maintaining a constant current through the electrolyte. The potentiostatic method is preferred to the galvanostatic method because which can control the selectivity of nitrate reduction at a given potential, causing only the thermodynamically favorable redox reaction to occur. The reaction occurs in a three-electrode electrochemical cell comprising working, reference, and counter electrodes (Garcia-Segura et al. 2018). The working electrode acts as the cathode, providing a platform for the exchange of electrons required for electrochemical nitrate reduction. The counter electrode helps to complete the circuit, and the reference electrode is used as a reference for the measurement and regulation of the working electrode's potential. All these electrodes are immersed in a conducting electrolyte solution. Working electrodes are coated with electrocatalysts that facilitate the redox reaction through a direct charge transfer.

All the measured potentials are referred against the standard hydrogen potential. Usually, electrolysis occurs when a potential greater than the theoretical potential, known as the overpotential, is applied. Therefore, low overpotential results in low activation energy and great electrocatalytic activity. Studies on the rational design and fabrication of electrocatalysts with low costs and maximum efficiency in the electroreduction of nitrate to ammonia are of great interest. Previous studies have shown that the main factors to be considered to have maximum efficiency are (1) the formation of favorable reaction intermediates for the selective

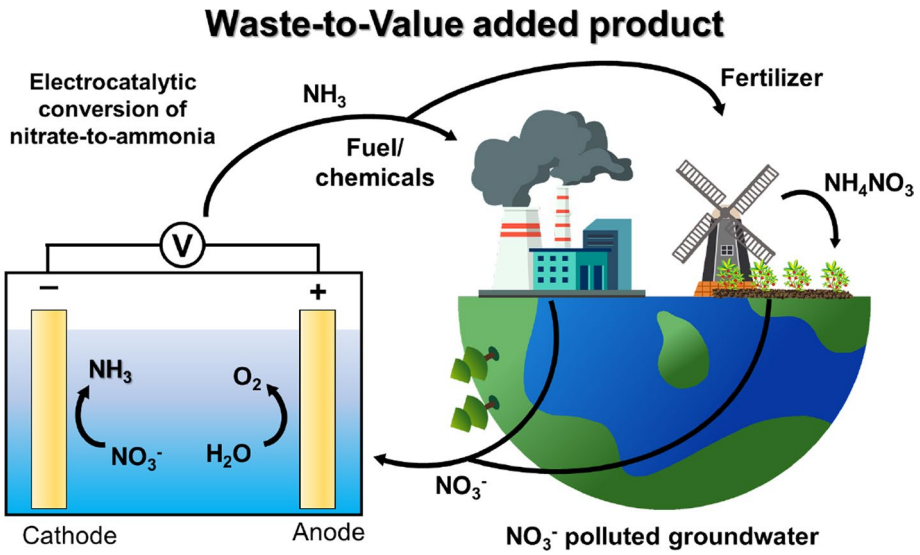

Fig. 2 The concept of waste-to-value added product: Electrocatalytic removal of nitrate as targeted pollutant from the industrial, agricultural waste contaminated groundwater and subsequently, selective production of ammonia as value-added product. The electrochemical cell mentioned with typical two-electrode system in a single compartment with anode and cathode, respectively, since the supporting electrolyte is same medium and pH. In the case of three-electrode system, we termed as counter, reference, and working electrode, respectively. Based on the potential window, the employed working electrode acts as anode or cathode, wherein electrochemical nitrate reduction reaction is mostly taking place on the negative potential window, so the working electrode is considered as cathode. However, we can also perform under H-cell setup where the supporting electrolyte is in different conditions

production of ammonia over other side reactions, (2) the dependence of the reactant concentration and the pH of the reaction medium, and (3) the selection of highly stable electrocatalysts that interact limitedly with the reaction intermediates, thus maximizing the electrocatalytic reduction capability (Wang et al. 2021d; Zhang et al. 2021).

Mechanistic aspects of electrocatalytic nitrate reduction

The mechanism of nitrate electroreduction involves complex multielectron reactions involving various stable nitrogen intermediates and products, such as ammonia, nitrite, hydrazine, hydroxylamine, nitric oxide, and nitrous oxide, whose oxidation states range from − 3 to + 5 (Wang et al. 2021d; Zhang et al. 2021). The involvement of various reaction intermediates complicates understanding the reaction mechanism operating at a given electrode surface. However, many factors and reaction conditions can affect selectivity and preferential pathways. High selectivity can be achieved when the elementary reactions and formation of various by-products are correctly understood.

Among the various reaction products, the most thermodynamically stable are dinitrogen and ammonia or ammonium. The conversion of nitrate to dinitrogen is a form of restoration of the disrupted nitrogen cycle, whereas the conversion of nitrate to ammonia at ambient reaction conditions introduces the concept of waste-to-wealth. Although the main focus of nitrate conversion is N_2 and NH_3 as stable products, as illustrated in Reactions (1) and (2), various factors, such as electrodes or crystal planes, can modify the final products (Zhang et al. 2021).

$$NO_3^- + 9\,H^+ + 8e^- \rightleftarrows NH_3 + 3\,H_2O \quad (1)$$

$E^\circ = -0.12$ V versus Standard hydrogen electrode

$$2\,NO_3^- + 12\,H^+ + 10\,e^- \rightleftarrows N_2 + 6\,H_2O \quad (2)$$

$E^\circ = 1.17$ V versus Standard hydrogen electrode.

The reaction mechanism is classified into direct electrocatalytic and indirect autocatalytic mechanisms (Min et al. 2021; Wang et al. 2021d). In the indirect autocatalytic mechanism, although the overall reaction is the conversion of nitrate to nitrous acid, there is no direct involvement of nitrate ions in the electron transfer reduction process. Rather, NO^+ or $NO_2^{\cdot}$ are the electroactive species, and they further initiate an autocatalytic mechanism. This mechanism mainly occurs in an acidic medium when the concentration of nitrate ions is greater than 1.0 M. Based on the two predominant electroactive species NO_2, NO_2^-, and NO^+, the indirect mechanism involves two pathways, namely, the Vetter and Schmid pathways (Wang et al. 2021d). Both pathways involve the production of nitrous acid using N_2O_4 through three elementary steps: (a) electron transfer, (b) intermediate step, and (c) production of nitrous acid.

1. Vetter pathway

   (a) Electron transfer

   $$NO_2 + e^- \rightarrow NO_2\cdot \quad (3)$$

   (b) Intermediate step

   $$NO_2\cdot + H^+ \rightleftharpoons HNO_2 \quad (4)$$

   (c) Production of nitrous acid

   $$HNO_2 + HNO_3 \rightarrow N_2O_4 + H_2O \quad (5)$$

   $$N_2O_4 + 2NO + 2H_2O \leftrightharpoons 4HNO_2 \quad (6)$$

2. Schmid pathway

   (a) Electron transfer

   $$NO^+ + e^- \rightarrow NO \quad (7)$$

   (b) Intermediate step

   $$HNO_2 + H^+ \rightarrow NO^+ + H_2O \quad (8)$$

   (c) Production of nitrous acid

   $$HNO_3 + HNO_2 \rightarrow N_2O_4 + H_2O \quad (9)$$

   $$N_2O_4 + 2NO + 2H_2O \rightleftharpoons 4HNO_2 \quad (10)$$

The second reaction mechanism for the electrochemical reduction of nitrate is the direct electrocatalytic reduction mechanism, which occurs in an alkaline medium that has a relatively low concentration of nitrate ions. The direct mechanism is usually followed when converting nitrate-containing wastewater effluents to ammonia, as these contain low concentrations of nitrate ions about less than 1.0 M (Min et al. 2021). The direct mechanism can proceed through the hydrogen-adsorbed and electron reduction pathways. The nitrate electroreduction is initiated by the adsorption of nitrate ions onto the cathodic electrode, but the adsorption of binary ions from the solution limits the overall reduction rate. Thus, electrocatalysts with an enhanced selective adsorption of nitrates with a large surface area for adsorption are an important parameter in electroreduction. The adsorbed NO_3^- is converted into nitrite through a three-step electrochemical–chemical–electrochemical process (Garcia-Segura et al. 2018). Subsequently, the nitrite is converted into nitric oxide ($NO_{(ads)}$). $NO_{(ads)}$ is an important

divergent-centered intermediate that branches out into different reactions to form dinitrogen and ammonia.

In the hydrogen-adsorbed pathway, the water molecules of the aqueous medium are reduced to H_{ads} and OH^- through the Volmer process (Reaction (11)).

$$H_2O + e^- \rightarrow H_{(ads)} + OH^- \quad (11)$$

Because of high reduction potential ($E^{\circ}_{(H^+/H^{\cdot})} = -2.31$ V versus standard hydrogen electrode), H_{ads} acts as a reducing agent and reduces several intermediates, such as adsorbed $NO_2^-(ads)$, $NO_{(ads)}$, $N_{(ads)}$, and $NH_{2(ads)}$, resulting in the formation of ammonia. Two $N_{(ads)}$ can react to form dinitrogen, but the reaction requires high activation energy of approximately 0.75 eV to form an N–N triple bond, which is greater than that of H_{ads} (0.10 eV) (Wang et al. 2021d). Additionally, the formation of the N–H bond initiated by H_{ads} is kinetically more favorable than that of the N–N bond. Therefore, the H_{ads} mediated pathway is selective for the formation of ammonia or ammonium. This pathway usually occurs at a relatively low operational potential and in the presence of noble metal-based electrocatalysts, such as Pt, Pd, Ru, and Ir, because of their high affinity to H_2 (Wen et al. 2022a; Zhang et al. 2021). Since the formation of the N – H bond mediated by $H_{(ads)}$ is more kinetically favorable than that of the N – N bond, the dominant end-product is ammonia. The detailed H_{ads} mediated pathway is shown from Reactions (12–18).

$$NO_3^-(aq) \rightarrow NO_3^-(aqs) \quad (12)$$

$$NO_3^-(ads) + 2H_{(ads)} \rightarrow NO_2^-(ads) + H_2O \quad (13)$$

$$NO_2^-(ads) + H_{(ads)} \rightarrow NO_{(ads)} + OH^- \quad (14)$$

$$NO_{(ads)} + 2H_{(ads)} \rightarrow N_{(ads)} + H_2O \quad (15)$$

$$N_{(ads)} + H_{(ads)} \rightarrow NH_{(ads)} \quad (16)$$

$$NH_{(ads)} + H_{(ads)} \rightarrow NH_{2(ads)} \quad (17)$$

$$NH_{2(ads)} + H_{(ads)} \rightarrow NH_{3(ads)} \quad (18)$$

In the electrocatalytic pathway, the formation of nitrite is the first step (Reaction (19)). The conversion of nitrate to nitrite is the rate-determining step (de Groot and Koper 2004); hence, the fundamental step in initiating charge transfer kinetics. Transition metal-based electrocatalysts with an unpaired d-electron, such as Cu, Ag, and Pt, can enhance reaction kinetics, as they have similar molecular orbital energies to those of nitrate. This similarity in their lowest unoccupied molecular orbital energies can help in the electron ejection required for the reduction to nitrite (Min et al. 2021). Furthermore, nitrite-to-nitric oxide reduction is a critical step in monitoring the formation of various products, such as ammonia, dinitrogen, and nitrous oxide.

$$NO_3^-(ads) + 2H^+ + 2e^- \rightarrow NO_2^-(ads) + H_2O \quad (19)$$

$$NO_{2(ads)} + 2H^+ + 2e^- \rightarrow NO_{(ads)} + H_2O \quad (20)$$

The existence of $NO_{(ads)}$ and in the solution $\left(NO_{(aq)}\right)$ can result in $N_2O_{(ads)}$ formation (Reactions (21) and (22)), which can further be reduced to N_2.

$$NO_{(ads)} + NO_{(aq)} + 2H^+ + 2e^- \rightarrow N_2O_{(ads)} + H_2O \quad (21)$$

$$N_2O_{(ads)} + 2H^+ + 2e^- \rightarrow N_2 + H_2O \quad (22)$$

The dissociation of $NO_{(ads)}$ into adsorbed nitrogen ($N_{(ads)}$) and the combination of the two $N_{(ads)}$ can also generate N_2 (Reactions (23) and (24)). However, this N_2 formation pathway has not been experimentally proven.

$$NO_{(ads)} + 2H^+ + 2e^- \rightarrow N_{(ads)} + H_2O \quad (23)$$

$$N_{(ads)} + N_{(ads)} \rightarrow N_2 \quad (24)$$

The interaction of $NO_{(ads)}$ with protons and electrons can also result in the formation of the intermediate azanone $HNO_{(ads)}$ (Reaction (25)). The ammonia formation pathway can be explained by the electrochemical–electrochemical mechanism (Garcia-Segura et al. 2018), which comprises two direct charge transfer reactions. Reaction (26), which involves the conversion of $NO_{(ads)}$ to $HNO_{(ads)}$, is the rate-determining step. Furthermore, the subsequent reactions will lead to the generation of hydroxylamine, and the electrochemical reduction of hydroxylamine will yield ammonia (Reactions (27) and (28)).

$$NO_{(ads)} + H^+ + e^- \rightarrow HNO_{(ads)} \quad (25)$$

$$HNO_{(ads)} + H^+ + e^- \rightarrow H_2NO_{(ads)} \quad (26)$$

$$H_2NO_{(ads)} + H^+ + e^- \rightarrow NH_2OH_{(ads)} \quad (27)$$

$$NH_2OH_{(ads)} + 2H^+ + 2e^- \rightarrow NH_3 + H_2O \quad (28)$$

From the above discussion, the several multielectron transfer reactions involve numerous intermediates and by-products. The identification and quantification of these stable, unstable, and instantaneous intermediates are necessary for understanding the fundamental reaction pathways

for the formation of desired products. Hence, identifying and fabricating suitable electrocatalytic materials for the reduction reaction with desirable products is achievable by understanding the fundamentals of the reaction mechanism.

Catalyst design and applications of nitrate-to-ammonia technology

Metal oxide-based electrocatalysts

Oxides mostly based on transition metals, such as Cu (combined or not with Co or Al or Mn or Pd), Co, Ag, Ti (doped or not with Pd), Nb, Bi, and Ru, with different interfaces, phases, structures, defects, and oxygen vacancies. have performed excellently as electrocatalysts in reducing nitrate to ammonia, showing great nitrate conversion efficiency, substantial ammonia yield or conversion, high Faradaic efficiency, and large ammonia selectivity. In this section, we present a summary of different oxides used in the electroreduction of nitrate to ammonia. Wang et al. (2020b) produced CuO nanowire arrays from the thermal treatment of $Cu(OH)_2$ nanowire arrays and observed the electrochemical reconstruction of CuO nanowire arrays to Cu-Cu_2O nanowire arrays, which served as the active phase in nitrate-to-ammonia reduction. The authors found that at an optimal potential of − 0.85 V versus reversible hydrogen electrode, the nitrate conversion rate was approximately 97.0%, the ammonia yield rate was 0.2449 mmol h^{-1} cm^{-2}, Faradaic efficiency was 95.8%, and the ammonia selectivity reached 81.2% in a 0.5 M Na_2SO_4 solution. Using density functional theory calculations, the authors suggested that the formation of the *NOH reaction intermediate is aided by the electron transfer occurring at the Cu-Cu_2O interface, which decreases the H_2 production competition.

Xu et al. (2022b), applied the hierarchical-defect approach to producing a low-content Pd (2.93 at%) incorporated into Cu_2O. This Pd incorporation provoked the structural formation of corner-etched octahedra (Fig. 3), cavity defects, and the appearance of surface oxygen vacancy defects. Additionally, this synergic effect of defects helped to promote nitrate adsorption, resulting in the N–O bond being weakened and the by-product formation being restricted. The authors claimed that the electrochemical reduction from part of Cu_2O to Cu^0 signified that the in situ occurrence of Cu^+ and Cu^0 acted as an active site for nitrate electroreduction and that the catalytic hydrogenation to produce ammonia would be provided by the Pd active sites, forming a Pd-H intermediate from the H ion adsorption. The authors found that the ammonia obtained from the electroreduction of nitrate at an optimum potential of − 1.3 V versus saturated calomel electrode had a yield of 925.11 μg h^{-1} mg_{cat}^{-1}, a Faradaic efficiency of 96.56%, and a maximum selectivity of 95.31% in a 0.5 M K_2SO_4 electrolyte solution. Wang et al. (2022a) produced different oxides, including Cu_2O, on an island-like Cu surface obtained from electrodeposition, which showed that at − 0.8 V versus reversible hydrogen electrode and in a 0.5 M Na_2SO_4 electrolyte solution, nitrate conversion reached 99.14%, Faradaic efficiency was 98.28%, and

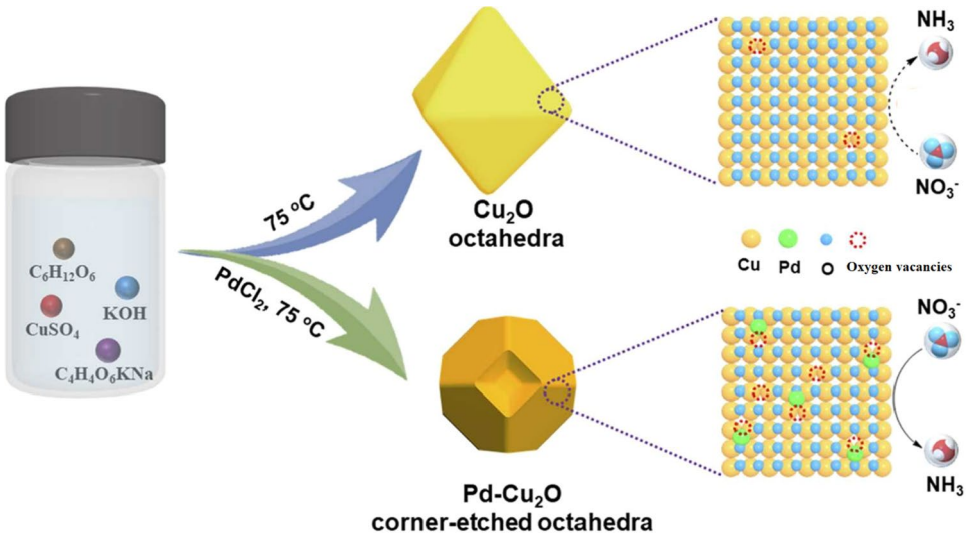

Fig. 3 Detailed schematic design for the fabrication of Pd incorporated Cu_2O. One-pot solution synthetic route involved for the preparation of Pd incorporated Cu_2O, wherein $PdCl_2$ was reduced to Pd(0) seeds by glucose and then catalyzed from Cu^{2+}-tartrate to Cu_2O octahedra by reductive transformation. Consequently, the Cu_2O octahedra grew into corner-etched octahedra Cu_2O via a Pd(0)-catalysis, the process is the so-called as oxygen-engaged oxidation method. During the reaction, Pd with low content was deposited on Cu_2O structure. Reproduced from reference (Xu et al. 2022b) with permission from Elsevier

selectivity toward ammonia production was 96.6%. Based on the density functional theory calculations, the authors suggested that the conversion of *HNOH to *HNHOH was promoted by the stable presence of Cu(I) at the Cu_2O surface and that the presence of oxygen atoms on this surface impedes H_2 coupling and the generation of by-products.

He et al. (2022) synthesized the core–shell Cu-CuO_x and Co-CoO phases on a Cu foil from binary Cu–Co sulfides through electrochemical redox activation. This electrocatalyst reduced nitrate to ammonia with a 90.6% Faradaic efficiency and 1.17 mmol h^{-1} cm^{-2} yield rate at − 0.175 V versus reversible hydrogen electrode in a 0.1 M KOH electrolyte solution, besides 36% of energy efficiency to a half-cell. The authors proposed that NO_3^- reduction to NO_2^- occurs preferentially in the inner Cu-CuO_x phase, whereas NO_2^- reduction to NH_3 occurs selectively in the outer-layer Co-CoO phase, both working together in tandem to produce ammonia. Fu et al. (2022) produced a Cu_2O-Cu interface on a Cu-based electrode through pulse electrodeposition and electroreduction. Furthermore, they applied this electrocatalyst in nitrate-to-ammonia reduction at − 0.25 V versus reversible hydrogen electrode in a 1 M KOH electrolyte solution, obtaining a yield rate of 2.17 mg h^{-1} cm^{-2}, a Faradaic efficiency of 84.36%, and a selectivity of 94.4%. The authors attributed the improved activity of the Cu_2O-Cu interface in the nitrate-to-ammonia reduction to the tuned mobility of NO_2^- in the interface and the electron transfer from the Cu-based electrocatalyst to NO_3^-. Jiang et al. (2022a) produced a strong metal-support interaction $Cu-Al_2O_3$ interface with Cu − O − Al bonds using CuAl mixed-oxide electroreduction. They found a 97.4% of ammonia selectivity to the $Cu_{52}Al_{48}$ catalyst, with 661.6 mg-N h^{-1} m^{-2} of specific activity, and 70.4% of Faradaic efficiency to ammonia production at − 1.10 V versus Ag–AgCl, 0.05 mM Na_2SO_4 of electrolyte solution, and when reducing 22.5 mg L^{-1} NO_3^-–N. The authors assumed that the $Cu^{\delta+}$ resulting from the Cu–O − Al bonds shows a great affinity to the N-intermediates, thus promoting the activation of the molecule and preventing intercoupling of the dinitrogen species.

Ren et al. (2021) produced Cu@$Cu_{2+1}O$ core-sheath nanowires contained at the surface concave–convex oxide layer) by drying Cu nanowires under air, which was achieved at − 1.2 V versus saturated calomel electrode in a 0.5 M K_2SO_4 electrolyte solution, an NO_3^- − N conversion rate of 78.57%, ammonia selectivity of 76%, Faradaic efficiency of 87.07%, and ammonia yield rate of 576.53 μg h^{-1} mg_{cat}^{-1}. The authors assumed that the electron transfer was facilitated by the metallic Cu components in the core, although the high density of the catalytic active sites was due to concave-convex $Cu_{2+1}O$ layers on the exterior. Additionally, the intermediates' adsorption energies during the nitrate reduction were modulated by the electronic interaction between Cu-$Cu_{2+1}O$ and the interface effect, which tunes the d-band center of Cu. Wang et al. (2021a) synthesized ultrathin heterostructured nanosheet arrays of Cu-oxygen vacancy-rich Cu-Mn_3O_4 on a Cu foam using the hydrothermal method, which was achieved at − 1.3 V versus saturated calomel electrode in a 0.5 M K_2SO_4 electrolyte solution, a 95.8% nitrate conversion, 87.6% selectivity, 92.4% Faradaic efficiency, and 0.21 $mmolh^{-1}$ cm^{-2} ammonia production rate. The authors assumed that the numerous oxygen vacancies and Cu-Cu-Mn_3O_4 interfaces modulated the electronic structure of the surface, promoting nitrate adsorption and nitrate-to-ammonia electroreduction.

Wang et al. (2021b) synthesized nanosheets of CoO_x with numerous adsorbed oxygen species at a potential of − 0.3 V versus reversible hydrogen electrode and a maximum ammonia production of 82.4 ± 4.8 mg h^{-1} mg_{cat}^{-1} or 36.62 mg h^{-1} cm^{-2} from the reduction of nitrate at 0.1 M KOH and 93.4 ± 3.8% Faradaic efficiency. Using density functional theory calculations, the authors assumed that the adsorbed oxygen improved the H_2 adsorption, which restrained the H_2 evolution reaction, thus favoring a more exothermic reaction pathway. Yu et al. (2020) synthesized nanosheet arrays of Co–CoO through electrodeposition and annealing methods, which electrocatalyzed the nitrate-to-ammonia reduction with a 93.8% Faradaic efficiency, 91.2% selectivity, and 194.46 μmol h^{-1} cm^{-2} yield rate at − 1.3 V versus saturated calomel electrode in a 0.1 M Na_2SO_4 electrolyte solution. The authors concluded that the Schottky-rectifying effect prompted the Co to CoO electron transfer, which resulted in a Co electron deficiency that obliterated the H_2 production and prevented the by-product formation due to their high energy barriers. Liu et al. (2021a) produced oxide-derived Ag through a square-wave pulse potential applied on an Ag foil, which worked as a selective electrocatalyst in NO_3^- − to − NO_2^- or NO_3^- − to − NH_4^+, depending on the cathodic potential applied where potential exceeded the theoretical charge of 116 C, NO_3^- − to − NH_4^+. They achieved an 89% Faradaic efficiency to NH_4^+ at − 1.35 V versus Ag–AgCl in a 0.1 M KCl electrolyte solution.

Jia et al. (2020) produced nanotubes of TiO_2 with oxygen vacancies, TiO_{2-x}, by heating in a H_2 atmosphere and found that the conversion of nitrate to ammonia at − 1.6 V versus saturated calomel electrode in a 0.5 M Na_2SO_4 electrolyte solution had a 95.2% conversion rate, 87.1% ammonia selectivity, 0.045 mmol h^{-1} mg^{-1} yield rate, and 85% Faradaic efficiency. The experimental H-cell setup for the nitrate-to-ammonia technology over the TiO_2 catalyst is depicted in Fig. 4. The authors assumed that the oxygen atom from the nitrate occupied the oxygen vacancies existing at TiO_{2-x}, weakening the N − O bond and limiting the formation of by-products. Guo et al. (2021) produced nanorod arrays of Pd-doped TiO_2 on carbon cloth using the ion exchange method, which reached a 99.6% nitrate conversion efficiency, 92.1%

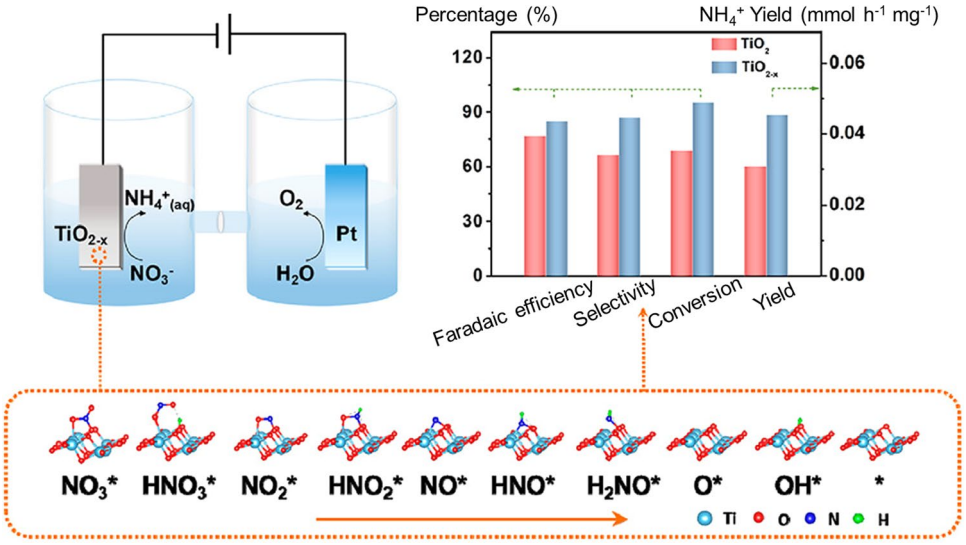

Fig. 4 Typical H-cell experimental setup for the electrochemical conversion of nitrate to ammonia over the TiO_2 catalyst, and the resulting removal efficiency of nitrate and ammonium yield production with selectivity. The fabricated TiO_2 and TiO_{2-x} electrocatalysts on carbon cloth substrate employed as working electrode, along with saturated calomel electrode and platinum foil as reference and counter electrodes, respectively. 50 ppm of nitrate solution in 0.5 M Na_2SO_4 served as supporting electrolyte. The optimal TiO_{2-x} electrocatalyst exhibited an enhanced nitrate conversion rate of 95.2%, ammonium production yield of 0.045 $mmolh^{-1}$ $mg.^{-1}$, and Faradaic efficiency of 85% along with selectivity of 87.1%. Reproduced from reference (Jia et al. 2020) with permission from American Chemical Society

Faradaic efficiency, and 1.12 mg h^{-1} cm^{-2} ammonia yield rate at − 0.7 V versus reversible hydrogen electrode in a 1 M LiCl electrolyte solution. The authors concluded that the introduction of Pd heteroatoms induced TiO_2 lattice enlargement, which decreased the function of the catalyst surface, diminishing the intermediate adsorption energy.

Wan et al. (2022) constructed a NbO_x catalyst containing oxygen vacancies using hydrothermal and annealing methods that showed a 94.5% Faradaic efficiency and 55.0 μg h^{-1} $mg_{cat}{}^{-1}$ formation rate to ammonia from the nitrate reduction at − 1.15 V versus reversible hydrogen electrode in a 0.5 M K_2SO_4 electrolyte solution. The authors assumed that the NbO_x activity was due to the nature and the oxygen vacancies, which improve the key intermediates' binding energies. Chen et al. (2021) produced Bi_2O_3 nanosheets grown in situ on carbon cloth using the hydrothermal method, which reached an 84.9% nitrate reduction efficiency and an 80.3% ammonia selectivity after treatment for 180 min and a 10 mA cm^{-2} current density in a 0.5 M Na_2SO_4 electrolyte solution. The authors assumed that atomic H* and the direct electron transfer were responsible for the ammonia produced from the nitrate electroreduction. Wang et al. (2022c) grew nanosheets of amorphous RuO_2 on a carbon paper surface through annealing of the salt method, which reached 97.46% Faradaic efficiency and 96.42% ammonia selectivity from nitrate electroreduction in a 0.5 M Na_2SO_4 electrolyte solution. The authors concluded that the enriched oxygen vacancies at amorphous RuO_2 due to the disordered atomic distribution at a-RuO_2 adjusted the H_2 affinity and *d*-band center, decreasing the required energy to the speed-determining step of $NH_2^* \rightarrow NH_3^*$ for ammonia production. The summary of metal oxide-based electrocatalysts in the performance of nitrate reduction for ammonia production is presented in Table 1.

Metal alloys

A brief summary of the different kinds of alloys used in nitrate-to-ammonia electroreduction based on CuNi, CuPd, CuAu, CoP, and PtRu is discussed in this section. Wang et al. (2020a) produced a $Cu_{50}Ni_{50}$ alloy through electrodeposition and converted nitrate to ammonia with an Faradaic efficiency of 99 ± 1% at around − 0.15 V versus reversible hydrogen electrode in a 1.0 M KOH electrolyte solution. The authors suggested that the $Cu_{50}Ni_{50}$ alloy catalyst *d*-band center upshifted toward the Fermi level, enhancing the intermediates' adsorption energies. They also suggested that the insertion of Ni atoms displaced the potential-dependent step from the adsorption of NO_3^- to $^*NH_2$ hydrogenation due to the improved adsorption energy of NO_3^- to the surface of CuNi alloy, resulting in an overpotential diminution. Zhang et al. (2022b) prepared a Cu(111) surface containing atomically dispersed Au in small amounts with Cu vacancies through galvanic replacement and dealloying. This catalyst exhibited a Faradaic efficiency of 98.7% and a production rate of 555 μg h^{-1} cm^{-2} at − 0.2 V versus reversible hydrogen electrode in a 0.1 M KOH electrolyte solution to reduce nitrate to ammonia. The authors assumed that the isolated

Table 1 Overview of metal oxide and alloy-based catalysts, potentials, nitrate conversion efficiency, ammonia yields or production rates, Faradaic efficiencies, ammonia selectivity, and electrolyte solutions involved in the electrochemical reduction of nitrate

Catalyst	Potential	Nitrate conversion efficiency (%)	Ammonia yield or production rate	Faradaic efficiency (%)	Ammonia selectivity (%)	Electrolyte	Reference
Cu-Cu_2O NWAs	− 0.85 V vs. RHE	97.0	0.2449 mmol h^{-1} cm^{-2}	95.8	81.2	0.5 M Na_2SO_4	Wang et al. 2020b
Pd-Cu_2O	− 1.3 V vs. SCE	–	925.11 μg h^{-1} mg_{cat}^{-1}	96.56	95.31	0.5 M K_2SO_4	Xu et al. 2022b
Cu_2O	− 0.8 V vs. RHE	99.14		98.28	96.6	0.5 M Na_2SO_4	Wang et al. 2022a
Cu-CuO_x and Co-CoO	− 0.175 V vs. RHE	–	1.17 mmol h^{-1} cm^{-2}	90.6	–	0.1 M KOH	He et al. 2022
CuAl	− 1.10 V vs. Ag–AgCl	–	661.6 mg-N h^{-1} m^{-2}	70.4	97.4	0.05 mM Na_2SO_4	Jiang et al. 2022a
Cu@$Cu_{2+1}O$	− 1.2 V vs. SCE	78.57	576.53 μg h^{-1} mg_{cat}^{-1}	76	87.07	0.5 M K_2SO_4	Ren et al. 2021
Cu-Cu-Mn_3O_4	− 1.3 V vs. SCE	95.8	0.21 mmol h^{-1} cm^{-2}	92.4	87.6	0.5 M K_2SO_4	Wang et al. 2021a
CoO_x	− 0.3 V vs. RHE	-	82.4 ± 4.8 mg h^{-1} mg_{cat}^{-1} (36.62 mg h^{-1} cm^{-2})	93.4 ± 3.8	–	0.1 M KOH	Wang et al. 2021b
Oxide-derived Ag	− 1.35 V vs. Ag–AgCl	–	–	89	–	0.1 M KCl	Liu et al. 2021a
Cu_2O-Cu	− 0.25 V vs. RHE	–	2.17 mg h^{-1} cm^{-2}	84.36	94.4	1 M KOH	Fu et al. 2022
TiO_{2-x}	− 1.6 V vs. SCE	95.2	0.045 mmol h^{-1} mg^{-1}	85	87.1	0.5 M Na_2SO_4	Jia et al. 2020
NbO_x	− 1.15 V vs. RHE	–	55.0 μg h^{-1} mg_{cat}^{-1}	94.5	–	0.5 M K_2SO_4	Wan et al. 2022
Co-CoO	− 1.3 V vs. SCE	–	194.46 μmol h^{-1} cm^{-2}	93.8	91.2	0.1 M Na_2SO_4	Yu et al. 2020
Bi_2O_3	–	84.9	–	–	80.3	0.5 M Na_2SO_4	Chen et al. 2021
a-RuO_2	–	–	–	97.46	96.42	0.5 M Na_2SO_4	Wang et al. 2022c
Pd-TiO_2	− 0.7 V vs. RHE (Guo et al. 2021)	99.6	1.12 mg h^{-1} cm^{-2}	92.1	–	1 M LiCl	
$Cu_{50}Ni_{50}$ alloy	− 0.15 V vs. RHE	99 ± 1			–	1 M KOH	Wang et al. 2020a
V_{Cu}-Au_1Cu	− 0.2 V vs. RHE	–	555 μg h^{-1} cm^{-2}	98.7	–	0.1 M KOH	Zhang et al. 2022b
Co-P@Ti	− 0.6 V vs. RHE	86.9	416.0 ± 7.2 mg h^{-1} cm^{-2}	93.6 ± 3.3	–	0.2 M Na_2SO_4	Li et al. 2021d
$Pt_{78}Ru_{22}$-carbon	–	–	–	93	–	1 M H_2SO_4	Wang et al. 2021i
CuPd(3:1)	− 0.46 V vs. RHE	95.27	784.37 mg h^{-1} mg_{cat}^{-1}	90.02	77.49	0.5 M K_2SO_4	Xu et al. 2021
PdCu-Cu_2O	− 0.80 V vs. RHE	99.82	0.190 mmol h^{-1} cm^{-2}	94.32	96.70	0.5 M Na_2SO_4	Yin et al. 2021
$Pt_{75}Ru_{25}$-carbon	0.1 V vs. RHE	–	–	93	–	pH 1	Wang et al. 2021h

NWAs nanowire arrays; *vs.* versus; *RHE* reversible hydrogen electrode; *SCE* saturated calomel electrode; *a-RuO_2* amorphous RuO_2

Au atoms and neighboring Cu vacancies were responsible for regulating the geometric structure and local electronic at the surface of the catalyst, facilitating *NH_3 desorption and the H_2O to *H activation to advance the kinetic energy hydrogenation of NO_3^-.

Li et al. (2021d) produced a cobalt-phosphorous alloy film supported at the Ti plate using electrodeposition and found a yield rate of 416.0 ± 7.2 mg h^{-1} cm^{-2} and an Faradaic efficiency of 93.6 ± 3.3% at − 0.6 V versus reversible hydrogen electrode in a 0.2 M Na_2SO_4 electrolyte solution, with a conversion rate of 86.9% after 10 h of bulk electrolysis to reduce nitrate to ammonia. The authors assumed that as the transition metal phosphide showed a high ability for H-adsorption, they can active catalytically hydrogenation reactions. Furthermore, the amorphous structure of Co-P, which is rich in defects, showed a high density of catalytic sites. Xu et al. (2021) synthesized aerogels of Cu3Pd1 by alloying Pd with Cu using the wet chemical method and co-reducing the metal precursors with $NaBH_4$. At − 0.46 V versus reversible hydrogen electrode in a 0.5 M K_2SO_4 electrolyte solution, the Cu3Pd1 aerogels showed a 95.27% NO_3^- conversion rate, 77.49% selectivity, 90.02% Faradaic efficiency to ammonia, and 784.37 mg h^{-1} mg_{cat}^{-1} ammonia production rate. The authors assumed that Pd alloying adjusted the Cu *d*-band center, favoring the nitrate and related intermediates' adsorption energies at the Cu sites during the electroreduction of nitrate. Additionally, the Pd sites may have acted as active centers for H-atom adsorption, which accumulated at the catalyst surface of the hydrogenated species and promoted NH_3 formation. Yin et al. (2021) synthesized PdCu-Cu_2O mesoporous hollow sphere hybrids containing highly dispersed PdCu alloys and an ultrathin Cu_2O shell by heating Cu_2O cubes and Pd salt in an aqueous solution, which reached a 99.82% nitrate conversion rate, 96.70% selectivity, 94.32% Faradaic efficiency, and 0.190 mmol h^{-1} cm^{-2} ammonia yield rate at − 0.80 V versus reversible hydrogen electrode in a 0.5 M Na_2SO_4 electrolyte solution (Fig. 5). The authors concluded that the highly dispersed PdCu alloys adjusted the synthesis path of Cu_2O ammonia production due to the change of nitrate in the adsorption sites, which blocked the generation of the

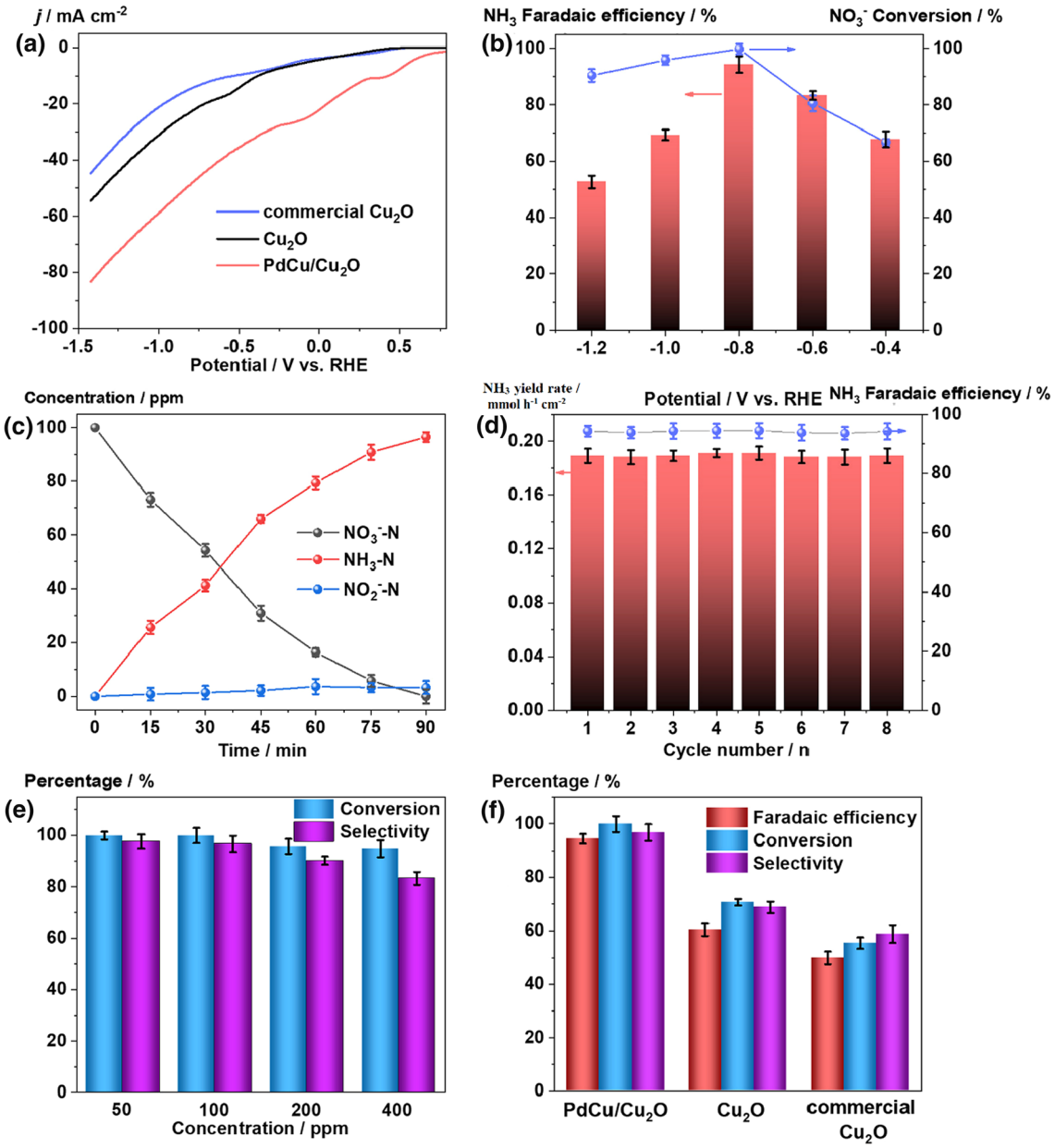

Fig. 5 Electrochemical nitrate reduction reaction over the PdCu-Cu_2O catalyst. **A** Linear sweep voltammetry curves in a 0.5 M Na_2SO_4 electrolyte, **B** Faradaic efficiencies of the ammonia generation and nitrate removal rate at different applied potentials, **C** change in the concentrations of nitrate, nitrite, and ammonia changes with respect to time, **D** ammonium production yield alongside the Faradaic efficiency for eight consecutive cycles, **E** ammonia selectivity and nitrate conversion with different initial concentrations of the nitrate solution, and **F** conversion rate of nitrate and the selectivity and Faradaic efficiency of ammonia generation over commercial Cu_2O, synthesized Cu_2O, and PdCu-Cu_2O catalysts. Thus, the obtained plot revealed that the optimal PdCu-Cu_2O catalysts exhibited highest electrochemical nitrate reduction performance when compare to commercial Cu_2O and synthesized pure Cu_2O materials. The optimal potential for the electrochemical reduction reaction over PdCu-Cu_2O catalysts was −0.8 V versus reversible hydrogen electrode which showed an enhanced ammonia yield and Faradaic efficiency with highest selectivity. RHE—reversible hydrogen electrode; ppm—parts per million; vs. —versus. Reproduced from reference (Yin et al. 2021) with permission from Elsevier

*NOH intermediate and facilitated the formation of the *N intermediate.

Wang et al. (2021h) compared the conversion of nitrate to ammonia using PtRu alloys and thermocatalytic and electrocatalytic methods. The $Pt_{75}Ru_{25}$-C was synthesized using $NaBH_4$ chemical reduction of metal salt precursors, showing the optimal nitrate conversion rate when H_2 pressure is increased from 0.1 to 1 atm H_2 and the potential is changed from 0.15 to 0.05 V versus reversible hydrogen electrode. At 0.1 V versus reversible hydrogen electrode,

the Faradaic efficiency in ammonia production reached 93% at a pH of 1 and 54% at a pH of 7. The authors concluded that increasing the content of Ru in the alloy increased the adsorption strengths of nitrate, H_2, and the intermediates. Wang et al. (2021i) synthesized Pt_xRu_y alloy nanoparticles on vulcan carbon using the $NaBH_4$ reduction method and found Faradaic efficiency to be higher than 93% in nitrate-to-ammonia reduction in a 1.0 M H_2SO_4 electrolyte solution. The authors attributed the improved reduction of nitrate to ammonia using an alloying effect on the nitrate and H_2 binding energies such as the binding of the intermediates to the $Pt_{78}Ru_{22}$-vulcan carbon catalyst are either not too strong or not too weak. The alloys based at CuNi, CuPd, CuAu, CoP, and PtRu were shown to be effective electrocatalysts for nitrate reduction to ammonia, achieving high nitrate conversion efficiency, considerable ammonia yield or conversion, large Faradaic efficiency, and great ammonia selectivity. The summary of metal alloy-based electrocatalysts in the performance of nitrate reduction for ammonia production is presented in Table 1.

Non-oxide electrocatalysts

Because of high efficiency and eco-friendliness, the elimination of NO_3^- through electrocatalytic reduction has become a promising technique. However, during the electrocatalytic reduction, the metal oxides and alloy-based catalysts were applied as the electrodes in the consecutive reduction pathway of NO_3^-, and N_2 and NH_3 evolved as products, which is a point of concern (Balaji et al. 2021; Das et al. 2022). Other important aspects to be considered are the high dependence of the selectivity and reactivity on the electrode category applied and the medium pH. For example, in the reduction of NO_3^-, Pd and Pt have exhibited favorable selectivity in producing N_2O, N_2 gaseous components, and NH_3 (Gootzen et al. 1997). However, in the selective reduction of NO_3^- to $NH_3{\cdot}H_2O$, Pd has shown superior activity (Pintar et al. 2004). However, the prohibitive cost and scarcity of Pd have restricted large-scale usage in wastewater purification techniques. However, in this section, we elaborate on non-oxide catalysts and their future scopes in the electrocatalytic reduction process.

Metal phosphides

Because of their low cost, hybrid orbitals, and superior electronic conductivity, metal phosphides or transition metal phosphides are decent candidates and have shown impressive electrocatalytic activity. Nickel phosphide is a frequently utilized electrocatalyst for examining activity in H_2 evolution reaction and oxygen evolution reaction, among others. (Liu et al. 2018; Popczun et al. 2013; Roberts et al. 2018; Stern et al. 2015). In a recent study, both NO_3^- reduction and HER were examined using a cathode made of nickel phosphide fabricated on carbon cloth where the generated active *H recombined with each other and helped in reducing NO_3^-, which finally led to the relatively low efficiency of the nitrate electrocatalytic reduction (Huo et al. 2020b). Yao et al. (2021) fabricated nickel phosphide with (111) facets on nickel foam and applied them as a self-supporting electrode for nitrate reduction to synthesize NH_3 with excellent Faradaic efficiency of 99.23% and a high production yield rate of 0.056 mmol h^{-1} mg^{-1}. Additionally, the as-prepared cathode exhibited high selectivity for NH_3 of 89.1%. Cobalt phosphide is another electrocatalyst utilized in NO_x^- reduction to ammonia (Zhang et al. 2022a).

Recently, Zhang et al. (2022a) tested the electrocatalytic conversion of nitrate to NH_3 in an alkaline medium using a cathode formed with cobalt phosphide on a carbon cloth substrate. The as-prepared nanowire catalyst exhibited a high Faradaic efficiency and conversion rate and showed durable stability and a low onset potential for NO_x^- reduction. Another group utilized Mg^{2+} ion-doped calcium carbonate nanoshuttles to develop amorphous and porous cobalt phosphide nanoshuttles through precipitation, followed by a high-temperature phosphidation process (Fig. 6 i) (Jia et al. 2021). The electrocatalysts exhibited a high ammonia yield rate of 19.28 ± 0.53 mg h^{-1} mg^{-1} and Faradaic efficiency of $94.24\% \pm 2.8\%$. The authors specifically illustrated that the shuttle-like morphology of the synthesized material has proven beneficial for the electrocatalytic application (Fig. 6 ii). The amorphous crystal structure, porous architecture, and improved surface area are responsible for the enhanced ammonia production rate (Jia et al. 2021). Another amorph of CoP with high-quality nanorings has also exhibited a high ammonia yield of 30.1 mg h^{-1} mg^{-1} with an Faradaic efficiency of 97.1% toward nitrate-to-ammonia conversion (Hong et al. 2021b). A few beneficial features of the catalyst highlighted in the article were its high surface area, substantial coordinately unsaturated active sites, and available mass transfer pathways, all highlighted by the authors as the characteristics responsible for enhanced ammonia production. Other aspects mentioned were high stability, high selectivity, and an earlier onset reduction potential. In another study, Wu and Yu (2021) illustrated the pathway of Ru-doped CO_2P monolayers, which were thermodynamically stable, and the Gibbs free energy for NO_3^- adsorption was made to be more negative than that of the proton, with an electrode potential of -0.5 V.

In recent studies (Liang et al. 2022; Wen et al. 2022b; Ye et al. 2022), nanosheet arrays of both cobalt and nickel phosphide were developed by different groups, which almost exhibited a 90%–100% Faradaic efficiency and a great ammonia-evolving rate. Wu et al. (2021a) recently investigated the potential of transition metal-doped hexagonal boron phosphide in nitrate reduction using a theoretical

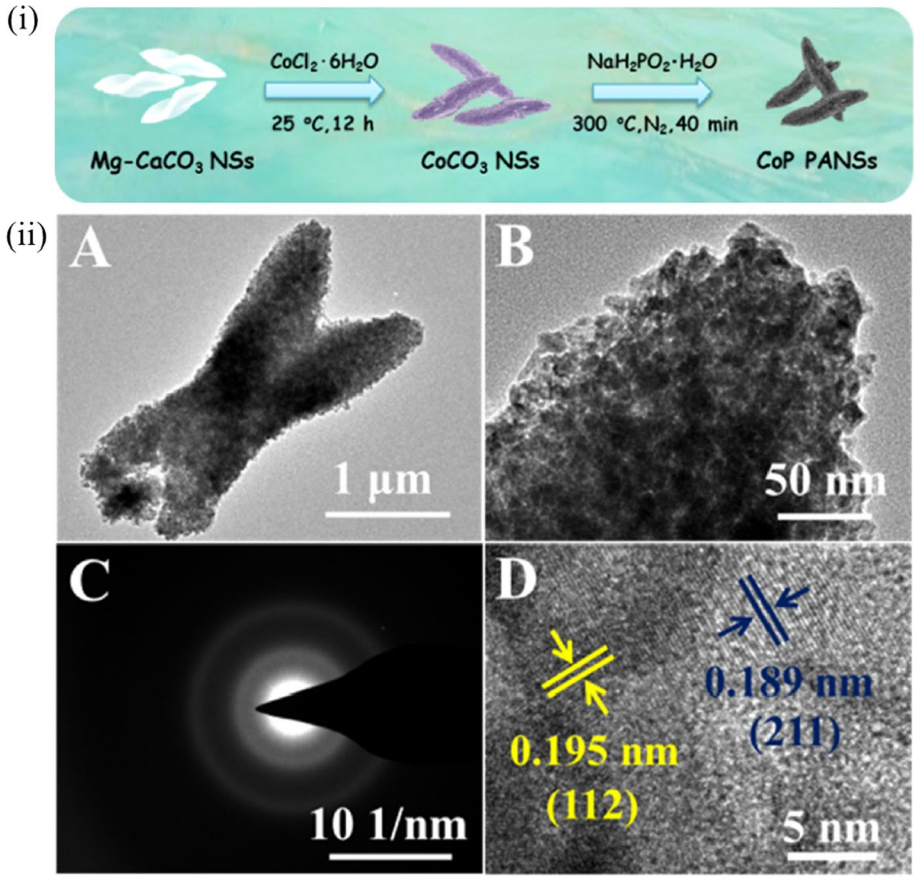

Fig. 6 (i) Fabrication procedure of Mg-doped porous and amorphous CoP nanoshuttles (Mg-CoP PANSs) through precipitation, followed by a high-temperature phosphidation process. (ii) TEM and SAED patterns of Mg-CoP PANSs. At first, the Mg-$CaCo_3$ nanoshuttles as precursor was synthesized by the solution mixture of $MgCl_2$ and $CaCl_2$ in the existence of polyethylene glycol as a surfactant. Then, the two-step synthesis route followed to synthesis CoP nanoshuttles via the simple precipitation of Mg-$CaCo_3$ to $CoCo_3$ nanoshuttles, followed by high-temperature phosphidation treatment to obtain CoP nanoshuttles product. Reproduced from reference (Jia et al. 2021) with permission from American Chemical Society. NSs—nanoshuttles; PANSs—porous and amorphous nanoshuttles

approach. This monolayer compound showed superior electronic and mechanical characteristics and acted favorably as a substrate for a single atom catalyst. The catalyst seemed facile for synthesis and had high thermal stability, which is suitable for experimental studies. However, electrocatalysts such as FeCoP, WP, FeP, and NiP have already been examined as H_2 evolution reaction catalysts and should be explored for nitrate reduction (Kibsgaard et al. 2015; Laursen et al. 2015; McEnaney et al. 2014; Xu et al. 2013).

Metal sulfides

In recent studies, various reduced sulfur compounds, such as H_2S and FeS, were examined as electron donors for the reduction of nitrate to ammonia. Garcia-Gil (1996) presented in their investigation that the addition of NO_3^- to sulfide-containing freshwater sediments, in both laboratory and natural conditions, results in the oxidation of sulfide and the concomitant accumulation of ammonia. The report also explained that the NO_3^- reduction pathway represents up to 30% of the total nitrate reduction in sulfide-dependent ammonia production. Molybdenum sulfide is another electrocatalyst considered suitable for nitrate-to-ammonia electrocatalytic reduction, over an extensive pH range ~ 3–11 (Li et al. 2016b). The onset potential for the pH dependence denitrification shows that the high activity was due to the ability of molybdenum sulfide to induce a concerted proton-electron transfer, signifying a turnover frequency comparable to that of Mo-dependent nitrate reductases. The protonated Mo–S reductive species can facilitate the nitrate and nitrite activation by establishing H_2 bonds among the substrates and active sites. Sato et al. (1999) investigated the impact of titanate on CdS nanocomposites toward nitrate reduction. Moreover, the catalytic activity greatly improved when the Pt nanoparticles were doped in the interlayer of the composite and furthermore, when methanol was added and acted as a sacrificial hole acceptor suitable for endorsing the NO_3^- reduction.

Metal carbides

Reports on utilizing transition metal carbides for electrochemical nitrate reduction are available (Xu et al. 2022a). The carbides with an unoccupied d-orbital exhibited a strong adsorption ability toward NO_3^-. Meanwhile, the sp-hybridized state of the transition metal in the carbides moves to the center of the surface with the *d*-state of the transition metal and the s-state of carbon. The excessively occupied orbital offers precise prospects for reverse donation to the p-orbital of N_2, which benefits the activation of the N- to

O-triple bond with improved nitrate reduction activity. One of the extensively utilized electrochemical nitrate reduction catalysts for easy NH_3 synthesis and NO_3^- removal is iron carbide of Fe_3C phase. The excellent electronic structure and morphology enable the carbide to activate the catalytic sites and prevent sluggish kinetics. Wang et al. (2021a, b, c, d, e, f, g, h, i) reported that Fe_3C nanoflakes embedded in N-doped carbon nanosheets possess a high surface area of 860.024 $m^2\ g^{-1}$ for superior selectivity and nitrate reduction. At − 0.5 V, the NH_3 yield, Faradaic efficiency, selectivity, and current density reached 1.19 mmol $h^{-1}\ mg^{-1}$, 96.7%, 79.0%, and 85.6 mA cm^{-2}, respectively, exceeding most reported results. Such exceptional performances mainly originated from the optimized electronic structures that optimized nitrate adsorption and the reaction kinetics with Tafel slope of 56.7 mV dec^{-1}. The NO_3^- reduction to NH_3 occurs through NO_2^-, where the Fe^{3+}-Fe^{2+} ratios and d-band centers play a vital role as the rate-determining step (Wang et al. 2021e).

Samples, such as Mo_2C-based nanocomposites, are highly recommended for superior nitrogen reduction reaction, electrocatalytic ammonia synthesis, and H_2 evolution inhibition, which could be utilized for the nitrate reduction reaction (Cheng et al. 2018). The density functional theory and electronic state density simulation studies confirmed that carbides provide active center sites for nitrate reduction. Additionally, two-dimensional atomic layer MXenes have exhibited beneficial electrochemical nitrogen reduction reaction performance with numerous active transition metal sites, excellent ion transmission, satisfactory conductivity, and stability in aqueous solutions (Sun et al. 2019). Generally, MXenes are referred to as two-dimensional transition metal nitrides and carbides. Majorly, M_3C_2, M_2C, and M_4C_3 are the three carbides of MXenes frequently applied for nitrate-to-ammonia reduction. Nevertheless, the MXene synthesis environments and conditions are harsh, as preparation at ambient temperature and pressure is difficult. The easy oxidization of MXenes in air made many characteristics acquirable using calculation and simulation. Major efforts have been made to tune the geometric and electronic structures of MXenes for fast nitrate reduction performance. As one of the typical $M_3C_2T_x$ structures, $Ti_3C_2T_x$ is used in the electrocatalytic reduction of nitrate due to its mechanical flexibility and stability (Li et al. 2021c). Surface and interface engineering, doping, or alloying is preferred in carbides to adsorb more nitrates and improve catalytic conversion to ammonia.

Carbon-based electrocatalysts in nitrate reduction

Casella and Contursi (2014) combined rhodium particles and multiwalled carbon nanotubes in an sulfuric acid medium to examine the nitrate reduction performance in ammonia production. Thus, the Rh-catalytic sites sufficiently adsorbed NO_2^- ions. During the electrocatalytic activity, the alternating development of $Rh(OH)_n$ enabled the desirable desorption of fouling $Rh(NOx)_{ads}$ adsorbed species and conserved the initial electrocatalytic performance of the Rh nanoparticles. By contrast, the initial steps of the electrocatalytic nitrite reduction proceeded through the direct and competitive reaction mechanisms of adsorption and desorption of nitrite and H_2 species, respectively. The authors also tested the redox activity of gold particles dispersed into multiwalled carbon nanotubes (Casella et al. 2014). Similarly, the vast potential usage of Pd-Fe-multiwalled carbon nanotubes can also be explored, as they have already been used to examine the denitrification process (Wang et al. 2021g).

The electrochemical results and index correlation analysis confirmed that the electron exchange capacity ~ 1.401 mmol eg^{-1} of Pd-Fe-multiwalled carbon nanotubes is positively associated with a reduction in nitrite performance (Wang et al. 2019, 2020c). Similarly, Fe–Pd–Fe_3O_4-multiwalled carbon nanotubes have also been studied in nitrate reduction, where the NO_3^-–N was completely eliminated within 2 h, 39% and 25% of which were converted into NO_2^-–N and NH_4^+–N, respectively. Figure 7 shows the resulting nitrate reduction mechanism over the Fe–Pd–Fe_3O_4-multiwalled carbon nanotube catalyst (Wang et al. 2021f). The reusability and recoverability test of Fe–Pd–Fe_3O_4-multiwalled carbon nanotubes through five consecutive cycles showed that a 43% NO_3^-–N removal rate was reached, revealing that multiwalled carbon nanotubes prolonged the reduction efficiency of NO_3^-–N by controlling the aggregation of catalytic nanoparticles. Yin et al. (2022) fabricated a corrosion-resistant Cu-based catalyst through thermolysis of the Cu-salophen coordination organic polymer on multiwalled carbon nanotube wires. This experiment showed an N_2–N selectivity of 93% and efficient catalytic performance for NO_3–N, with a NO_3^-–N conversion yield of about 66% in Cl^--free neutral solution within 12 h. Furthermore, the study revealed that negligible Cu degradation occurred in continuous electrolysis for 60 h, and catalytic performance was not heavily deteriorated. The low Cu content ~ 1.6% and special core–shell structures enable this Cu@N-carbon catalyst to possess better corrosion-resistant properties in long-term electrolysis for nitrate reduction.

In another study, Liu et al. 2022a examined the ability of a nitrogen-doped carbon matrix in nitrate-to-ammonia reduction, where the Faradaic efficiency was found to be 79.6% and selectivity was almost 94.4%. Additionally, the density functional theory calculations revealed that both the electronic and geometric structures of the catalysts were improved because of the introduction of nickel into the modified copper lattice. The nickel and copper sites in the CuNi alloy activated synergistically to accelerate the NO_2* to HNO_2* hydrogenation and suppress the H_2 evolution reaction, enhancing the selective

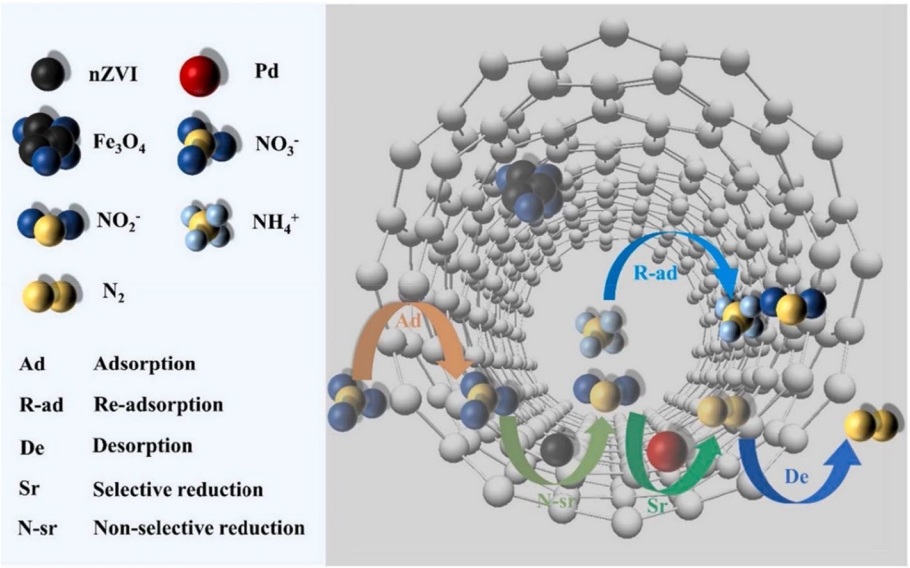

Fig. 7 Surface mechanism for the adsorption and electrochemical reduction of nitrate over the Fe–Pd–Fe_3O_4-multiwalled carbon nanotube catalyst. During nitrate reduction process, initially, adsorption takes place initially on the surface of metal active centers. Then, the adsorbed species get reduced at the surface of catalysts and followed by the re-adsorption which is known as removal process of ammonium product. Reproduced from reference (Wang et al. 2021f) with permission from Elsevier. nZVI—zero valent iron nanoparticles

production of ammonia. Nitrate conversion using this catalyst was found to be almost 81.2%. Duan et al. (2019) developed N-doped graphitic carbon-encapsulated iron nanoparticles that have shown long-term durability, high electrocatalytic activity, and 83% nitrate removal. The selectivity of nitrogen was ~ 25.0% in the absence of Cl^- and was enhanced to 100% when accompanied by NaCl ~ 1.0 gL^{-1}. Notably, there was no substantial difference at ~ 95% confidence interval in the percentage of removal measured over 20 cycles for the fabricated cathode where 20% iron was applied. The author further added that potential efforts can be made to improve selectivity and performance for nitrogen in the absence of Cl^- and that the upscaling strategy preparation of the catalyst should be advanced for nitrate control in wastewater treatment. Waste-derived carbon has also attracted many researchers in the nitrate reduction process. Li et al. (2021b) carbonized natural wood to prepare charcoal cathodes, which exhibited an ammonia production rate of 0.570 mmol L^{-1} h^{-1} cm^{-2}, a nitrate removal rate of 91.2%, and an outstanding selectivity of around 98.5% at an optimal − 3.6 V potential.

Metal–organic frameworks

The metal–organic frameworks are well known for their porous structure and high surface area. Two-dimensional and three-dimensional networks are easily constructed by altering the synthesis precursor of polydented organic ligands, linkers, and metal ions (Wang and Astruc 2020), which can vary the secondary building units or metal clusters. Different designs or metal frameworks can be implemented in various activities. Different metal–organic framework morphology-governed experiments in the selective catalytic reduction of nitrate to ammonia were conducted by Gao et al. (2021a). The performances varied due to the presence of active pores, catalytic sites, and stability in the acidic medium. The microporous and mesoporous metal–organic frameworks have surface areas up to 10,000 m^2g^{-1}, which provide a large platform for electrocatalytic reactions (Li et al. 2016a). Furthermore, researchers' investigations of the synergistic effect of metal–organic frameworks with conductive carbon bases, such as graphene or multi-walled carbon nanotubes, can be more conducive for electrocatalytic nitrate reduction to ammonia (Petit and Bandosz 2009). Hybrid nanocatalysts, such as heterometallic or nanocomposite metal–organic frameworks, can enhance catalytic reactions and gas absorption (Liu et al. 2022a).

The bridges and cavities in metal–organic frameworks can act as cushions for the transport and diffusion of products with a low mass transfer limit (Humphreys et al. 2018). A particular shape and size of the catalytic active sites in metal–organic frameworks are proven to be highly selective and sensitive to electrocatalytic nitrate reduction (Qin et al. 2022). The bridging ligands also contribute to the thermal and chemical stability during the adsorption of hazardous nitrates in wastewater treatment. Furtado et al. (2011) investigated Cu-benzene 1,3,5-tricarboxylate with an ordered mesoporous silica template for the stability of metal–organic frameworks during ammonia synthesis.

Thus, because of their excellent catalytic properties for adsorption, stability, sensitivity, and selective reduction of nitrates, metal–organic frameworks have been exponentially investigated by various researchers. For example, Li et al. (2016a) reported Cu- benzene 1,3,5-tricarboxylate as a selective low-temperature catalyst. The paddlewheel units with Cu^{2+} dimers produce a high number of metal sites for catalytic activity and also have good stability. Overall, the low amount of Pd in high surface area catalysts was examined to make the nanocatalyst cost-effective with

better catalyst performance (Xu et al. 2022b). The flawed, edge-etched Pd-CuO_2 octahedral structure was proven to have high electrochemical selectivity toward nitrate reduction. The dual active sites, cavity structure, and rich surface oxygen vacancies were found to be a scalable medium for ample ammonia synthesis. The high Faradaic efficiency of Cu-based metal–organic frameworks and nitrates may be due to the similarity in their molecular energy levels during the electroreduction reaction. Nitrate electroreduction suffers from the generation of by-products, such as nitrogen oxyions or H_2; thus, a selective catalyst is essential. To overcome this issue, Qin et al. (2022) reported Ni- metal–organic frameworks-supported Ru_xO_y clusters as having high selectivity for NH_4^+ and a high yield of ammonia. The study of selectivity was also supported by theoretical analysis, which stated that by-products such as NO_2 are easily converted to NH_4^+ and then to ammonia. A density functional theory calculation by Liu et al. 2022a proved that the insertion of Cu into Ni sites and a supported nitrogen-doped carbon base could improve the ammonia yield by suppressing H_2 evolution (Fig. 8). Interestingly, Gao et al. (2021b) investigated a Cu^{II}-bipyridine-based thorium metal–organic framework for NH_3 storage through electroreduction reaction with a 92.5% Faradaic efficiency and a 225.3 μmol h^{-1} cm^{-2} yield. The low capacity and recyclability of nanocatalysts hinder the usability of NO_3^- to NH_3 in electroreduction. In that context, metal–organic frameworks supported with graphene oxide composites in a sandwich-like structure can maintain structural and chemical stability (Petit and Bandosz 2009).

The interconnected bonds and porousness of metal–organic frameworks and graphene oxide enhance ammonia intake. Besides Cu-metal–organic frameworks, Materials Institute Lavoisier-100(Fe) is known for the catalytic conversion of nitrate to ammonia due to the redox nature of iron species (Wang et al. 2014). The different metal-loaded metal–organic frameworks have been proven to be more effective catalysts than regular catalysts due to the synergistic effect of metal ions, metal–organic

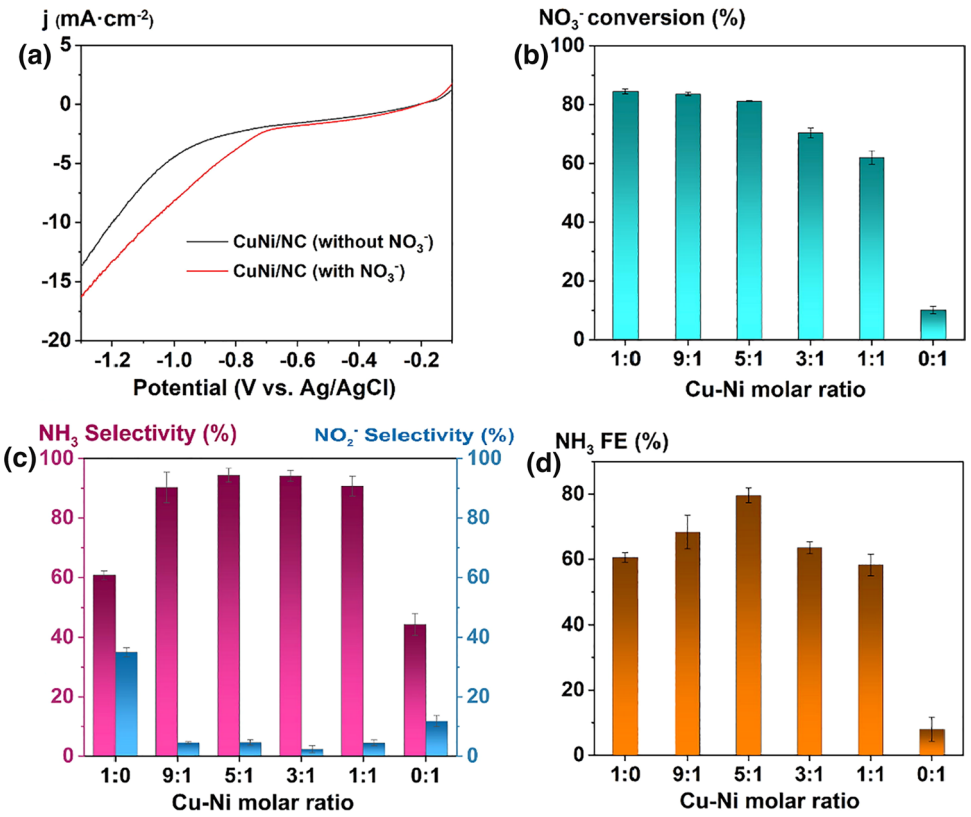

Fig. 8 Electrocatalytic nitrate reduction activity of CuNi alloy embedded in an N-doped carbon matrix (CuNi-NC) obtained by the pyrolysis of bimetallic metal–organic frameworks. **a** Linear sweep voltammetry curves of CuNi-NC in a 1.0 M phosphate-buffered saline solution with and without nitrate, the resulting **b** nitrate removal efficiency, and **c** and **d** ammonia and nitrate selectivity with differing ratios of Cu and Ni in the CuNi-nitrogen-doped carbon catalyst. Overall, the linear sweep voltammetry indicates that the current density was enhanced by adding nitrate into the supporting electrolyte confirms the active response of CuNi-nitrogen-doped carbon electrocatalyst for the electrocatalytic reduction of nitrate. The optimal Cu5Ni1 exhibited an enhanced electrochemical reduction reaction with highest ammonia product selectivity with Faradic efficiency. NC—nitrogen-doped carbon; FE—Faradaic efficiency. Reproduced from reference (Liu et al. 2022a) with permission from Elsevier

frameworks (Mounfield et al. 2016; Zhang et al. 2017), and metal–organic framework-derived oxide nanocatalysts such as Mn-doped Fe_2O_3 derived from a bimetallic metal–organic framework and also act as good avenues for the catalytic removal of nitrates (Lee and Kwak 2018). Such studies provide a scope for further investigation of other metal–organic framework-derived nanocatalysts for cost-effective and eco-friendly nitrate reduction.

Recently, zirconia-based metal–organic framework has been studied for the high gas uptake capacity (Binaeian et al. 2021). A stable and electroactive Zr-metal–organic framework with Zr_6-nanoclusters and redox-reversible tetrathiafulvalene derivatives as inorganic nodes and organic linkers, respectively, was explored using metal nanodots where M = Pd, Ag, or Au. Among the metal-nanodots-Zr-metal–organic framework catalysts, Pd-nanodots-Zr-metal–organic framework was found to have a high ammonia yield due to the high porosity, conductivity, and efficiency, which enhance the mass transport process (Jiang et al. 2022c). Hence, the various metal-based metal–organic frameworks exhibit extraordinary feasibility for electrochemical nitrate-to-ammonia technology. Metal–organic frameworks are also recognized for the photocatalytic reduction of nitrate and aid in the green synthesis of ammonia (Choi et al. 2019; Wang et al. 2022b). Table 2 presents the summary of non-oxide electrocatalysts toward the performance of nitrate reduction in ammonia production.

Perspective

Various types of wastewater were investigated to find the most convenient reaction demands. The resultant studies proved that the wastewater effluents must contain a minimum concentration of nitrate. A high level of nitrate concentration was found in nuclear wastewater effluents, whereas a low concentration was found in industrial and polluted groundwater, among others. Although polluted groundwater contains nitrate levels unfit for human consumption, the removal through electroreduction is not conducive due to the low nitrate concentration, neutral pH conditions, and low ionic conduction. Consequently, additional steps have to be installed to increase the concentration of nitrate

Table 2 Summary of non-oxide-based catalysts, potentials, nitrate conversion efficiencies, ammonia yields or production rates, Faradaic efficiency, ammonia selectivity, and electrolyte solutions involved in the electrochemical reduction of nitrate

Catalyst	Potential V vs. RHE	Nitrate conversion efficiency (%)	Ammonia yield or production rate	Faradaic efficiency (%)	Ammonia selectivity (%)	Electrolyte	References
Ni_2P-carbon cloth	− 0.7 to 0.0	53.1	NA	NA	NA	0.5 M H_2SO_4	(Huo et al. 2020b)
Ni_2P-Ni foam	NA	64.2	32.7 mg L^{-1}	NA	NA	0.5 M H_2SO_4, 1 M PBS, and 1 M KOH	(Huo et al. 2020a)
MoAl boride	0 to − 0.35 V	NA	9.2 μg h^{-1} cm^{-2} mg^{-1}	30.1%	NA	0.1 M KOH	(Fu et al. 2020)
Fe-Fe_3C	0.2415 V vs. NHE	98	NA	NA	95%	NaCl and Na_2SO_4	(Lan et al. 2020)
CuNi-NC	− 1.0 V	81.2	NA	79.6	94.4	0.1 M PBS	(Liu et al. 2022a)
RuNi-MOF	− 1.7 V vs. Ag–AgCl	NA	274 mg h^{-1} mgcat.$^{-1}$	73%	100	Na_2SO_4 and $NaNO_3$	(Qin et al. 2022)
Zr-MOF	− 1.3	NA	287.31 mmol·h^{-1}·g^{-1} cat	58.1	NA	0.1 M Na_2SO_4	(Jiang et al. 2022b)
Polymeric g-C_3N_4	− 1.6 V vs. SCE	72.52	0.03262 $mmol^{-1}$ g^{-1} h^{-1}	89.96	69.78	0.5 M Na_2SO_4	(Huang et al. 2021)
CoP nanorings	− 0.5 V		30.1 mg h^{-1} mg^{-1} cat	97.1	–	0.5 M Na_2SO_4	(Hong et al. 2021a)
Cu@Th-BPYDC MOF	− 0.1 V vs. RHE		225.3 μmol h^{-1} cm^{-2}	92.5	–	1.0 M KOH + 100 mM KNO_3	(Gao et al. 2021c)
Fe single atom	− 0.66 vs. RHE		20,000 μg h^{-1} mgcat.$^{-1}$	75	–	K_2SO_4-KNO_3	(Wu et al. 2021b)
Carbon-coated Cu nanoparticles MOFs	− 0.2 V vs. RHE		487.8 mmol g^{-1} cat h^{-1}	94.2	–	1.0 M KOH	(Hu et al. 2021)

NC nitrogen-doped carbon; *MOF* metal–organic framework; *g-C_3N_4* graphitic carbon nitride; *BPYDC* 2,2 0-bipyridine-5,5 0-dicarboxylate; *vs.* versus; *RHE* reversible hydrogen electrode; *NA* not available

ions before the reduction process. Various factors, such as the presence of contaminants like hexavalent chromium and a high chemical oxygen demand, can be challenging to the reduction process. The side reaction of water electrolysis, producing H_2 in large quantities, can lead to the risk of explosion. Hence, the removal of H_2 or transient utilization must be thoroughly studied. The surface modulation of the electrocatalysts can be applied as a remedial strategy to enhance product selectivity over H_2 evolution reaction, as the electrocatalyst with negatively adsorbed charged species is expected to reduce the H_2 evolution reaction. For example, oxygen- or chlorine-based anions adsorbed on the copper electrocatalyst can capture protons and suppress H_2 evolution reaction while significantly promoting cathodic nitrate reductions. Electrode materials have a direct role in the reaction kinetics and the product selectivity of electrochemical reduction. The catalyst materials for nitrate removal should possess selective adsorption properties toward electron-rich N and O species for enhanced conversion to ammonia. Studies have shown that nitrate is a more suitable source for ammonia than dinitrogen, as a low dissociation energy ~ 204 kJ mol^{-1} and greater solubility in aqueous solvents.

For future energy, the potential of selective nitrate-to-ammonia electroreduction can be summarized by the recent developments of efficient electrocatalysts with long-term stability. Transition metal-based electrocatalysts that exhibit variable oxidation states can enhance their electrocatalytic performance. The class of metal alloy-based electrocatalysts has the unique property of altering the charge distribution, making them suitable candidates for nitrate reduction. Transition metals with occupied d-orbitals having similar energy levels to that of the nitrate lowest unoccupied molecular orbital can significantly facilitate the electron transfer process. Beyond electrochemical performance, attention also needs to be paid to energy efficiency for proper electrode selection. Copper-based electrodes with unique electronic structures have proved to be the electrocatalysts of choice with optimal activity in an alkaline medium, but they lack long-term stability. Based on the concept of the green electro-conversion process, the development of economical and carbon-based materials must be explored. Selectivity and Faradaic efficiency are still challenging because of the complex reaction mechanism involving an eight-electron reduction course and competitive H_2 evolution reaction. Highly efficient and selective electrocatalysts for the large-scale production of ammonia from nitrate-containing wastewater remain lacking, providing plenty of research opportunities.

Conclusion

The versatile utilization of ammonia in manufacturing fertilizers and in chemical industries, as well as the recent exploration as a substitute energy carrier source, has increased the significance and production in the past few decades. The application of ammonia as a renewable energy carrier plays an important role as a carbon-free energy carrier and as a promising means for the efficient and economical indirect storage and transportation of H_2 energy. The direct conversion of ammonia in fuel cells can result in power generation. Nevertheless, the prevailing conventional production methods of ammonia, such as from the Haber–Bosch process and natural gas feedstock, result in the emission of greenhouse gases, which can be rectified by the waste-to-wealth concept reviewed here. Nitrate-containing wastewater effluents as a source for the electrochemical conversion of nitrate into ammonia results in value-added products at ambient reaction conditions. This method can be associated with the zero emission of greenhouse gases when the power supply is derived from renewable energy resources, which facilitates the removal of the nitrate pollutant from the wastewater and aids the restoration of the disrupted nitrogen cycle. The mechanistic aspects in electrocatalytic nitrate reduction is reviewed, along with the recent progress on the various electrocatalysts in the nitrate-to-ammonia conversion applications. Transition metals with occupied d-orbitals having similar energy levels to that of the nitrate lowest unoccupied molecular orbital can significantly facilitate the electron transfer process in the electrochemical nitrate reduction reaction.

Acknowledgements The authors acknowledge the financial support from National Research Foundation of Korea (NRF), (2022R1A2C2010686, 2019H1D3A1A01071209, 2021R1I1A1A01060380), and Korea Basic Science Institute (National research Facilities and Equipment Center) grant funded by the Ministry of Education. (No. 2019R1A6C1010042, 2021R1A6C103A427). This work is also supported by CAPES-PRINT (Grant 88881.311799/2018-01) and the Coordenação de Aperfeiçoamento de Pessoal de Nível Superior (CAPES—Finance Code 001). E.S.F.C is grateful to CAPES for the individual fellowship granted in support of their research. The author, Arun Prasad Murthy acknowledges VIT for providing VIT SEED GRANT (No. SG20210143) for carrying out this research work.

Declarations

Conflict of interest No conflicts of interest to declare.

References

Balaji TE, Tanaya Das H, Maiyalagan T (2021) Recent trends in bimetallic oxides and their composites as electrode materials for supercapacitor applications. ChemElectroChem 8(10):1723–1746. https://doi.org/10.1002/celc.202100098

Barrera L, Bala Chandran R (2021) Harnessing photoelectrochemistry for wastewater nitrate treatment coupled with resource recovery. ACS Sustain Chem Eng 9(10):3688–3701. https://doi.org/10.1021/acssuschemeng.0c07935

Binaeian E, Li Y, Yuan D (2021) Improving ammonia uptake performance of zirconium-based metal-organic frameworks through

open metal site insertion strategy. Chem Eng J 421:129655. https://doi.org/10.1016/j.cej.2021.129655
Casella IG, Contursi M (2014) Highly dispersed rhodium particles on multi-walled carbon nanotubes for the electrochemical reduction of nitrate and nitrite ions in acid medium. Electrochim Acta 138:447–453. https://doi.org/10.1016/j.electacta.2014.05.125
Casella IG, Contursi M, Toniolo R (2014) A non-enzymatic carbohydrate sensor based on multiwalled carbon nanotubes modified with adsorbed active gold particles. Electroanalysis 26(5):988–995. https://doi.org/10.1002/elan.201300644
Chen M, Bi J, Huang X, Wang T, Wang Z, Hao H (2021) Bi_2O_3 nanosheets arrays in-situ decorated on carbon cloth for efficient electrochemical reduction of nitrate. Chemosphere 278:130386. https://doi.org/10.1016/j.chemosphere.2021.130386
Cheng H, Ding LX, Chen GF, Zhang L, Xue J, Wang H (2018) Molybdenum carbide nanodots enable efficient electrocatalytic nitrogen fixation under ambient conditions. Adv Mater 30(46):e1803694. https://doi.org/10.1002/adma.201803694
Choi H, Peters AW, Noh H, Gallington LC, Platero-Prats AE, DeStefano MR, Rimoldi M, Goswami S, Chapman KW, Farha OK, Hupp JT (2019) Vapor-phase fabrication and condensed-phase application of a MOF-node-supported iron thiolate photocatalyst for nitrate conversion to ammonium. ACS Appl Energy Mater 2(12):8695–8700. https://doi.org/10.1021/acsaem.9b01664
Das HT, Balaji TE, Dutta S, Das N, Maiyalagan T (2022) Recent advances in MXene as electrocatalysts for sustainable energy generation: a review on surface engineering and compositing of MXene. Int J Energy Res. https://doi.org/10.1002/er.7847
de Groot MT, Koper MTM (2004) The influence of nitrate concentration and acidity on the electrocatalytic reduction of nitrate on platinum. J Electroanal Chem 562(1):81–94. https://doi.org/10.1016/j.jelechem.2003.08.011
Duan W, Li G, Lei Z, Zhu T, Xue Y, Wei C, Feng C (2019) Highly active and durable carbon electrocatalyst for nitrate reduction reaction. Water Res 161:126–135. https://doi.org/10.1016/j.watres.2019.05.104
Fu Y, Richardson P, Li K, Yu H, Yu B, Donne S, Kisi E, Ma T (2020) Transition metal aluminum boride as a new candidate for ambient-condition electrochemical ammonia synthesis. Nano-Micro Lett 12(1):65. https://doi.org/10.1007/s40820-020-0400-z
Fu W, Hu Z, Zheng Y, Su P, Zhang Q, Jiao Y, Zhou M (2022) Tuning mobility of intermediate and electron transfer to enhance electrochemical reduction of nitrate to ammonia on Cu_2O/Cu interface. Chem Eng J 433:133680. https://doi.org/10.1016/j.cej.2021.133680
Furtado AMB, Liu J, Wang Y, LeVan MD (2011) Mesoporous silica–metal organic composite: synthesis, characterization, and ammonia adsorption. J Mater Chem 21(18):6698–6706. https://doi.org/10.1039/c1jm10451a
Gao R, Zhang G, Ru X, Xu C, Li M, Lin R, Wang Z (2021a) Morphology control of metal-organic frameworks by Co-competitive coordination strategy for low-temperature selective catalytic reduction of NO with NH_3. J Solid State Chem 297:122031. https://doi.org/10.1016/j.jssc.2021.122031
Gao Z, Lai Y, Tao Y, Xiao L, Zhang L, Luo F (2021b) Constructing well-defined and robust Th-MOF-supported single-site copper for production and storage of ammonia from electroreduction of nitrate. ACS Cent Sci 7(6):1066–1072. https://doi.org/10.1021/acscentsci.1c00370
Garcia-Gil J (1996) Brunet RC, Garcia-Gil LJ. Sulfide-induced dissimilatory nitrate reduction to ammonia in anaerobic freshwater sediments. FEMS Microbiol Ecol 21: 131–138. FEMS Microbiol Ecol 21:131–138
Garcia-Segura S, Lanzarini-Lopes M, Hristovski K, Westerhoff P (2018) Electrocatalytic reduction of nitrate: fundamentals to full-scale water treatment applications. Appl Catal B Environ 236:546–568. https://doi.org/10.1016/j.apcatb.2018.05.041
Gootzen JFE, Peeters PGJM, Dukers JMB, Lefferts L, Visscher W, van Veen JAR (1997) The electrocatalytic reduction of NO_3^- on Pt, Pd and Pt + Pd electrodes activated with Ge. J Electroanal Chem 434(1–2):171–183. https://doi.org/10.1016/s0022-0728(97)00093-4
Guo Y, Zhang R, Zhang S, Zhao Y, Yang Q, Huang Z, Dong B, Zhi C (2021) Pd doping-weakened intermediate adsorption to promote electrocatalytic nitrate reduction on TiO_2 nanoarrays for ammonia production and energy supply with zinc–nitrate batteries. Energy Environ Sci 14(7):3938–3944. https://doi.org/10.1039/D1EE00806D
Hasan MH, Mahlia TM, Mofijur M, Rizwanul Fattah IM, Handayani F, Ong HC, Silitonga AS (2021) A comprehensive review on the recent development of ammonia as a renewable energy carrier. Energies. https://doi.org/10.3390/en14133732
He W, Zhang J, Dieckhöfer S, Varhade S, Brix AC, Lielpetere A, Seisel S, Junqueira JRC, Schuhmann W (2022) Splicing the active phases of copper/cobalt-based catalysts achieves high-rate tandem electroreduction of nitrate to ammonia. Nat Commun 13(1):1129. https://doi.org/10.1038/s41467-022-28728-4
Hong Q-L, Zhou J, Zhai Q-G, Jiang Y-C, Hu M-C, Xiao X, Li S-N, Chen Y (2021a) Cobalt phosphide nanorings towards efficient electrocatalytic nitrate reduction to ammonia. Chem Commun 57(88):11621–11624. https://doi.org/10.1039/D1CC04952F
Hong QL, Zhou J, Zhai QG, Jiang YC, Hu MC, Xiao X, Li SN, Chen Y (2021b) Cobalt phosphide nanorings towards efficient electrocatalytic nitrate reduction to ammonia. Chem Commun (camb) 57(88):11621–11624. https://doi.org/10.1039/d1cc04952f
Hu Q, Qin Y, Wang X, Zheng H, Gao K, Yang H, Zhang P, Shao M, He C (2021) Grain boundaries engineering of hollow copper nanoparticles enables highly efficient ammonia Electrosynthesis from Nitrate. CCS Chem. https://doi.org/10.31635/ccschem.021.202101042
Huang Y, Long J, Wang Y, Meng N, Yu Y, Lu S, Xiao J, Zhang B (2021) Engineering nitrogen vacancy in polymeric carbon nitride for nitrate electroreduction to ammonia. ACS Appl Mater Interfaces 13(46):54967–54973. https://doi.org/10.1021/acsami.1c15206
Humphreys L, Wilson I, McAteer D, Pons J (2018) Development of metal-organic framework (MOF) sensors for landmine detection. https://doi.org/10.5162/IMCS2018/P1AP.8
Huo S, Yang S, Niu Q, Song Z, Yang F, Song L (2020) Fabrication of porous configurated Ni_2P/Ni foam catalyst and its boosted properties for ph-universal hydrogen evolution reaction and efficient nitrate reduction. ChemCatChem 12(18):4600–4610. https://doi.org/10.1002/cctc.2020a00426
Huo S, Yang S, Niu Q, Yang F, Song L (2020) Synthesis of functional Ni2P/CC catalyst and the robust performances in hydrogen evolution reaction and nitrate reduction. Int J Hydrog Energy 45(7):4015–4025. https://doi.org/10.1016/j.ijhydene.2019.11.210
Jia R, Wang Y, Wang C, Ling Y, Yu Y, Zhang B (2020) Boosting selective nitrate electroreduction to ammonium by constructing oxygen vacancies in TiO_2. ACS Catal 10(6):3533–3540. https://doi.org/10.1021/acscatal.9b05260
Jia Y, Ji YG, Xue Q, Li FM, Zhao GT, Jin PJ, Li SN, Chen Y (2021) Efficient nitrate-to-ammonia electroreduction at cobalt phosphide nanoshuttles. ACS Appl Mater Interfaces 13(38):45521–45527. https://doi.org/10.1021/acsami.1c12512
Jiang G, Peng M, Hu L, Ouyang J, Lv X, Yang Z, Liang X, Liu Y, Liu H (2022) Electron-deficient Cuδ+ stabilized by interfacial Cu–O-Al bonding for accelerating electrocatalytic nitrate conversion. Chem Eng J 435:134853. https://doi.org/10.1016/j.cej.2022a.134853

Jiang M, Su J, Song X, Zhang P, Zhu M, Qin L, Tie Z, Zuo J-L, Jin Z (2022b) Interfacial reduction nucleation of noble metal nanodots on redox-active metal–organic frameworks for high-efficiency electrocatalytic conversion of nitrate to ammonia. Nano Lett 22(6):2529–2537. https://doi.org/10.1021/acs.nanolett.2c00446

Jiang M, Su J, Song X, Zhang P, Zhu M, Qin L, Tie Z, Zuo JL, Jin Z (2022c) Interfacial reduction nucleation of noble metal nanodots on redox-active metal-organic frameworks for high-efficiency electrocatalytic conversion of nitrate to ammonia. Nano Lett 22(6):2529–2537. https://doi.org/10.1021/acs.nanolett.2c00446

Kibsgaard J, Tsai C, Chan K, Benck JD, Nørskov JK, Abild-Pedersen F, Jaramillo TF (2015) Designing an improved transition metal phosphide catalyst for hydrogen evolution using experimental and theoretical trends. Energy Environ Sci 8(10):3022–3029. https://doi.org/10.1039/c5ee02179k

Lan Y, Chen J, Zhang H, Zhang W-x, Yang J (2020) Fe/Fe_3C nanoparticle-decorated N-doped carbon nanofibers for improving the nitrogen selectivity of electrocatalytic nitrate reduction. J Mater Chem A 8(31):15853–15863. https://doi.org/10.1039/D0TA02317E

Laursen AB, Patraju KR, Whitaker MJ, Retuerto M, Sarkar T, Yao N, Ramanujachary KV, Greenblatt M, Dismukes GC (2015) Nanocrystalline Ni_5P_4: a hydrogen evolution electrocatalyst of exceptional efficiency in both alkaline and acidic media. Energy Environ Sci 8(3):1027–1034. https://doi.org/10.1039/c4ee02940b

Lee J, Kwak SY (2018) Mn-doped maghemite (gamma-Fe_2O_3) from Metal-organic framework accompanying redox reaction in a bimetallic system: the structural phase transitions and catalytic activity toward NO_x removal. ACS Omega 3(3):2634–2640. https://doi.org/10.1021/acsomega.7b01865

Li C, Shi Y, Zhang H, Zhao Q, Xue F, Li X (2016a) Cu-BTC metal-organic framework as a novel catalyst for low temperature selective catalytic reduction (SCR) of NO by NH_3: promotional effect of activation temperature. Integr Ferroelectr 172(1):169–179. https://doi.org/10.1080/10584587.2016.1177385

Li L, Tang C, Cui X, Zheng Y, Wang X, Xu H, Zhang S, Shao T, Davey K, Qiao S-Z (2021) Efficient nitrogen fixation to ammonia through integration of plasma oxidation with electrocatalytic reduction. Angewandte Chem Int Edition 60(25):14131–14137. https://doi.org/10.1002/anie.2021a04394

Li X, Gu Y, Wu S, Chen S, Quan X, Yu H (2021b) Selective reduction of nitrate to ammonium over charcoal electrode derived from natural wood. Chemosphere 285:131501. https://doi.org/10.1016/j.chemosphere.2021.131501

Li Y, Ma J, Waite TD, Hoffmann MR, Wang Z (2021c) Development of a mechanically flexible 2D-MXene membrane cathode for selective electrochemical reduction of nitrate to N_2: mechanisms and implications. Environ Sci Technol 55(15):10695–10703. https://doi.org/10.1021/acs.est.1c00264

Li Y, Yamaguchi A, Yamamoto M, Takai K, Nakamura R (2016b) Molybdenum sulfide: a bioinspired electrocatalyst for dissimilatory ammonia synthesis with geoelectrical current. J Phys Chem C 121(4):2154–2164. https://doi.org/10.1021/acs.jpcc.6b08343

Li Z, Wen G, Liang J, Li T, Luo Y, Kong Q, Shi X, Asiri AM, Liu Q, Sun X (2021d) High-efficiency nitrate electroreduction to ammonia on electrodeposited cobalt–phosphorus alloy film. Chem Commun 57(76):9720–9723. https://doi.org/10.1039/D1CC02612G

Liang J, Hu W-F, Song B, Mou T, Zhang L, Luo Y, Liu Q, Alshehri AA, Hamdy MS, Yang L-M, Sun X (2022) Efficient nitric oxide electroreduction toward ambient ammonia synthesis catalyzed by a CoP nanoarray. Inorgan Chem Front 9(7):1366–1372. https://doi.org/10.1039/d2qi00002d

Liu H, Park J, Chen Y, Qiu Y, Cheng Y, Srivastava K, Gu S, Shanks BH, Roling LT, Li W (2021a) Electrocatalytic nitrate reduction on oxide-derived silver with tunable selectivity to nitrite and ammonia. ACS Catal 11(14):8431–8442. https://doi.org/10.1021/acscatal.1c01525

Liu T, Li A, Wang C, Zhou W, Liu S, Guo L (2018) Interfacial electron transfer of Ni_2 P-NiP_2 polymorphs inducing enhanced electrochemical properties. Adv Mater 30(46):e1803590. https://doi.org/10.1002/adma.201803590

Liu Y, Deng B, Li K, Wang H, Sun Y, Dong F (2022a) Metal-organic framework derived carbon-supported bimetallic copper-nickel alloy electrocatalysts for highly selective nitrate reduction to ammonia. J Colloid Interface Sci 614:405–414. https://doi.org/10.1016/j.jcis.2022.01.127

Liu Z, Wang C, Chen C, Li C, Guo C (2021) Selective electroreduction of nitrate to ammonia with high Faradaic efficiency on nanocrystalline silver. Electrochem Commun 131:107121. https://doi.org/10.1016/j.elecom.2021b.107121

Lu X, Song H, Cai J, Lu S (2021) Recent development of electrochemical nitrate reduction to ammonia: a mini review. Electrochem Commun 129:107094. https://doi.org/10.1016/j.elecom.2021.107094

Madhura L, Singh S, Kanchi S, Sabela M, Bisetty K (2019) Nanotechnology-based water quality management for wastewater treatment. Environ Chem Lett 17(1):65–121. https://doi.org/10.1007/s10311-018-0778-8

Martínez J, Ortiz A, Ortiz I (2017) State-of-the-art and perspectives of the catalytic and electrocatalytic reduction of aqueous nitrates. Appl Catal B Environ 207:42–59. https://doi.org/10.1016/j.apcatb.2017.02.016

McEnaney JM, Crompton JC, Callejas JF, Popczun EJ, Read CG, Lewis NS, Schaak RE (2014) Electrocatalytic hydrogen evolution using amorphous tungsten phosphide nanoparticles. Chem Commun (camb) 50(75):11026–11028. https://doi.org/10.1039/c4cc04709e

Min B, Gao Q, Yan Z, Han X, Hosmer K, Campbell A, Zhu H (2021) Powering the remediation of the nitrogen cycle: progress and perspectives of electrochemical nitrate reduction. Ind Eng Chem Res 60(41):14635–14650. https://doi.org/10.1021/acs.iecr.1c03072

Morin-Crini N, Lichtfouse E, Fourmentin M, Ribeiro ARL, Noutsopoulos C, Mapelli F, Fenyvesi É, Vieira MGA, Picos-Corrales LA, Moreno-Piraján JC, Giraldo L, Sohajda T, Huq MM, Soltan J, Torri G, Magureanu M, Bradu C, Crini G (2022) Removal of emerging contaminants from wastewater using advanced treatments. Rev Environ Chem Lett 20(2):1333–1375. https://doi.org/10.1007/s10311-021-01379-5

Mounfield WP, Taborga Claure M, Agrawal PK, Jones CW, Walton KS (2016) Synergistic effect of mixed oxide on the adsorption of ammonia with metal–organic frameworks. Ind Eng Chem Res 55(22):6492–6500. https://doi.org/10.1021/acs.iecr.6b01045

Mudhoo A, Paliya S, Goswami P, Singh M, Lofrano G, Carotenuto M, Carraturo F, Libralato G, Guida M, Usman M, Kumar S (2020) Fabrication, functionalization and performance of doped photocatalysts for dye degradation and mineralization: a review. Environ Chem Lett 18(6):1825–1903. https://doi.org/10.1007/s10311-020-01045-2

Petit C, Bandosz TJ (2009) MOF-graphite oxide composites: combining the uniqueness of graphene layers and metal-organic frameworks. Adv Mater 21(46):4753–4757. https://doi.org/10.1002/adma.200901581

Pintar A, Batista J, Muševič I (2004) Palladium-copper and palladium-tin catalysts in the liquid phase nitrate hydrogenation in a batch-recycle reactor. Appl Catal B 52(1):49–60. https://doi.org/10.1016/j.apcatb.2004.02.019

Popczun EJ, McKone JR, Read CG, Biacchi AJ, Wiltrout AM, Lewis NS, Schaak RE (2013) Nanostructured nickel phosphide as an electrocatalyst for the hydrogen evolution reaction. J Am Chem Soc 135(25):9267–9270. https://doi.org/10.1021/ja403440e

Prashantha Kumar TKM, Mandlimath TR, Sangeetha P, Revathi SK, Ashok Kumar SK (2018) Nanoscale materials as sorbents for nitrate and phosphate removal from water. Environ Chem Lett 16(2):389–400. https://doi.org/10.1007/s10311-017-0682-7

Qin J, Wu K, Chen L, Wang X, Zhao Q, Liu B, Ye Z (2022) Achieving high selectivity for nitrate electrochemical reduction to ammonia over MOF-supported Ru_xO_y clusters. J Mater Chem A 10(8):3963–3969. https://doi.org/10.1039/D1TA09441F

Ren T, Ren K, Wang M, Liu M, Wang Z, Wang H, Li X, Wang L, Xu Y (2021) Concave-convex surface oxide layers over copper nanowires boost electrochemical nitrate-to-ammonia conversion. Chem Eng J 426:130759. https://doi.org/10.1016/j.cej.2021.130759

Roberts EJ, Read CG, Lewis NS, Brutchey RL (2018) Phase directing ability of an ionic liquid solvent for the synthesis of HER-active Ni_2P nanocrystals. ACS Appl Energy Mater 1(5):1823–1827. https://doi.org/10.1021/acsaem.8b00213

Sato T, Ki S, Fujishiro Y, Yoshioka T, Okuwaki A (1999) Photochemical reduction of nitrate to ammonia using layered hydrous titanate/cadmium sulphide nanocomposites. J Chem Technol Biotechnol 67(4):345–349. https://doi.org/10.1002/(sici)1097-4660(199612)67:4%3c345::Aid-jctb586%3e3.0.Co;2-#

Shipman MA, Symes MD (2017) Recent progress towards the electrosynthesis of ammonia from sustainable resources. Catal Today 286:57–68. https://doi.org/10.1016/j.cattod.2016.05.008

Stern L-A, Feng L, Song F, Hu X (2015) Ni2P as a Janus catalyst for water splitting: the oxygen evolution activity of Ni_2P nanoparticles. Energy Environ Sci 8(8):2347–2351. https://doi.org/10.1039/c5ee01155h

Sun T, Zhang G, Xu D, Lian X, Li H, Chen W, Su C (2019) Defect chemistry in 2D materials for electrocatalysis. Mater Today Energy 12:215–238. https://doi.org/10.1016/j.mtener.2019.01.004

Valera-Medina A, Xiao H, Owen-Jones M, David WIF, Bowen PJ (2018) Ammonia for power. Prog Energy Combust Sci 69:63–102. https://doi.org/10.1016/j.pecs.2018.07.001

Velusamy K, Periyasamy S, Kumar PS, Vo D-VN, Sindhu J, Sneka D, Subhashini B (2021) Advanced techniques to remove phosphates and nitrates from waters: a review. Environ Chem Lett 19(4):3165–3180. https://doi.org/10.1007/s10311-021-01239-2

Wan X, Guo W, Dong X, Wu H, Sun X, Chu M, Han S, Zhai J, Xia W, Jia S, He M, Han B (2022) Boosting nitrate electroreduction to ammonia on NbO_x via constructing oxygen vacancies. Green Chem 24(3):1090–1095. https://doi.org/10.1039/D1GC04483D

Wang C, Ye F, Shen J, Xue K-H, Zhu Y, Li C (2022a) In situ loading of Cu_2O active sites on island-like copper for efficient electrochemical reduction of nitrate to ammonia. ACS Appl Mater Interfaces 14(5):6680–6688. https://doi.org/10.1021/acsami.1c21691

Wang F, Ding Q, Bai Y, Bai H, Wang S, Fan W (2022b) Fabrication of an amorphous metal oxide/p-$BiVO_4$ photocathode: understanding the role of entropy for reducing nitrate to ammonia. Inorgan Chem Front 9(4):805–813. https://doi.org/10.1039/d1qi01472b

Wang H, Mao Q, Ren T, Zhou T, Deng K, Wang Z, Li X, Xu Y, Wang L (2021a) Synergism of interfaces and defects: Cu/oxygen vacancy-rich Cu-Mn_3O_4 heterostructured ultrathin nanosheet arrays for selective nitrate electroreduction to ammonia. ACS Appl Mater Interfaces 13(37):44733–44741. https://doi.org/10.1021/acsami.1c11249

Wang J, Cai C, Wang Y, Yang X, Wu D, Zhu Y, Li M, Gu M, Shao M (2021b) Electrocatalytic reduction of nitrate to ammonia on low-cost ultrathin CoO_x nanosheets. ACS Catal 11(24):15135–15140. https://doi.org/10.1021/acscatal.1c03918

Wang J, Feng T, Chen J, Ramalingam V, Li Z, Kabtamu DM, He J-H, Fang X (2021) Electrocatalytic nitrate/nitrite reduction to ammonia synthesis using metal nanocatalysts and bio-inspired metalloenzymes. Nano Energy 86:106088. https://doi.org/10.1016/j.nanoen.2021c.106088

Wang P, Zhao H, Sun H, Yu H, Chen S, Quan X (2014) Porous metal–organic framework MIL-100(Fe) as an efficient catalyst for the selective catalytic reduction of NOx with NH_3. RSC Adv 4(90):48912–48919. https://doi.org/10.1039/c4ra07028c

Wang Q, Astruc D (2020) State of the Art and Prospects in Metal-organic framework (MOF)-based and MOF-derived nanocatalysis. Chem Rev 120(2):1438–1511. https://doi.org/10.1021/acs.chemrev.9b00223

Wang Y, Li H, Zhou W, Zhang X, Zhang B, Yu Y (2022) Structurally disordered RuO_2 nanosheets with rich oxygen vacancies for enhanced nitrate electroreduction to ammonia. Angewandte Chem Int Edition. https://doi.org/10.1002/anie.2022c02604

Wang Y, Wang C, Li M, Yu Y, Zhang B (2021d) Nitrate electroreduction: mechanism insight, in situ characterization, performance evaluation, and challenges. Chem Soc Rev 50(12):6720–6733. https://doi.org/10.1039/D1CS00116G

Wang Y, Xu A, Wang Z, Huang L, Li J, Li F, Wicks J, Luo M, Nam D-H, Tan C-S, Ding Y, Wu J, Lum Y, Dinh C-T, Sinton D, Zheng G, Sargent EH (2020a) Enhanced nitrate-to-ammonia activity on copper–nickel alloys via tuning of intermediate adsorption. J Am Chem Soc 142(12):5702–5708. https://doi.org/10.1021/jacs.9b13347

Wang Y, Zhang L, Niu Y, Fang D, Wang J, Su Q, Wang C (2021e) Boosting NH_3 production from nitrate electroreduction via electronic structure engineering of Fe_3C nanoflakes. Green Chem 23(19):7594–7608. https://doi.org/10.1039/D1GC01913A

Wang Y, Zhou W, Jia R, Yu Y, Zhang B (2020) Unveiling the activity origin of a copper-based electrocatalyst for selective nitrate reduction to ammonia. Angewandte Chem Int Edition 59(13):5350–5354. https://doi.org/10.1002/anie.201915992

Wang Z, Chen C, Liu H, Hrynshpan D, Savitskaya T, Chen J, Chen J (2019) Effects of carbon nanotube on denitrification performance of Alcaligenes sp. TB: promotion of electron generation, transportation and consumption. Ecotoxicol Environ Saf 183:109507. https://doi.org/10.1016/j.ecoenv.2019.109507

Wang Z, Chen C, Liu H, Hrynshpan D, Savitskaya T, Chen J, Chen J (2020) Enhanced denitrification performance of Alcaligenes sp. TB by Pd stimulating to produce membrane adaptation mechanism coupled with nanoscale zero-valent iron. Sci Total Environ 708:135063. https://doi.org/10.1016/j.scitotenv.2019.135063

Wang Z, Dai L, Yao J, Guo T, Hrynsphan D, Tatsiana S, Chen J (2021f) Enhanced adsorption and reduction performance of nitrate by Fe-Pd-Fe_3O_4 embedded multi-walled carbon nanotubes. Chemosphere 281:130718. https://doi.org/10.1016/j.chemosphere.2021.130718

Wang Z, Fu W, Hu L, Zhao M, Guo T, Hrynsphan D, Tatsiana S, Chen J (2021g) Improvement of electron transfer efficiency during denitrification process by Fe-Pd/multi-walled carbon nanotubes: Possessed redox characteristics and secreted endogenous electron mediator. Sci Total Environ 781:146686. https://doi.org/10.1016/j.scitotenv.2021.146686

Wang Z, Ortiz EM, Goldsmith BR, Singh N (2021h) Comparing electrocatalytic and thermocatalytic conversion of nitrate on platinum–ruthenium alloys. Catal Sci Technol 11(21):7098–7109. https://doi.org/10.1039/D1CY01075A

Wang Z, Young SD, Goldsmith BR, Singh N (2021) Increasing electrocatalytic nitrate reduction activity by controlling adsorption through PtRu alloying. J Catal 395:143–154. https://doi.org/10.1016/j.jcat.2020.12.031

Wen G, Liang J, Liu Q, Li T, An X, Zhang F, Alshehri AA, Alzahrani KA, Luo Y, Kong Q, Sun X (2022a) Ambient ammonia production via electrocatalytic nitrite reduction catalyzed by a CoP nanoarray. Nano Res 15(2):972–977. https://doi.org/10.1007/s12274-021-3583-9

Wen G, Liang J, Zhang L, Li T, Liu Q, An X, Shi X, Liu Y, Gao S, Asiri AM, Luo Y, Kong Q, Sun X (2022b) Ni_2P nanosheet array

for high-efficiency electrohydrogenation of nitrite to ammonia at ambient conditions. J Colloid Interface Sci 606(Pt 2):1055–1063. https://doi.org/10.1016/j.jcis.2021.08.050

Wu J, Li JH, Yu YX (2021a) Theoretical exploration of electrochemical nitrate reduction reaction activities on transition-metal-doped h-BP. J Phys Chem Lett 12(16):3968–3975. https://doi.org/10.1021/acs.jpclett.1c00855

Wu J, Yu Y-X (2021) Highly selective electroreduction of nitrate to ammonia on a Ru-doped tetragonal Co2P monolayer with low-limiting overpotential. Catal Sci Technol 11(21):7160–7170. https://doi.org/10.1039/d1cy01217g

Wu Z-Y, Karamad M, Yong X, Huang Q, Cullen DA, Zhu P, Xia C, Xiao Q, Shakouri M, Chen F-Y, Kim JY, Xia Y, Heck K, Hu Y, Wong MS, Li Q, Gates I, Siahrostami S, Wang H (2021b) Electrochemical ammonia synthesis via nitrate reduction on Fe single atom catalyst. Nat Commun 12(1):2870. https://doi.org/10.1038/s41467-021-23115-x

Xiang X, Guo L, Wu X, Ma X, Xia Y (2012) Urea formation from carbon dioxide and ammonia at atmospheric pressure. Environ Chem Lett 10(3):295–300. https://doi.org/10.1007/s10311-012-0366-2

Xu S, Kwon H-Y, Ashley DC, Chen C-H, Jakubikova E, Smith JM (2019) Intramolecular hydrogen bonding facilitates electrocatalytic reduction of nitrite in aqueous solutions. Inorg Chem 58(14):9443–9451. https://doi.org/10.1021/acs.inorgchem.9b01274

Xu W, Yu C, Chen J, Liu Z (2022) Electrochemical hydrogenation of biomass-based furfural in aqueous media by Cu catalyst supported on N-doped hierarchically porous carbon. Appl Catal B Environ 305:121062. https://doi.org/10.1016/j.apcatb.2022a.121062

Xu Y, Ren K, Ren T, Wang M, Liu M, Wang Z, Li X, Wang L, Wang H (2021) Cooperativity of Cu and Pd active sites in CuPd aerogels enhances nitrate electroreduction to ammonia. Chem Commun 57(61):7525–7528. https://doi.org/10.1039/D1CC02105B

Xu Y, Ren K, Ren T, Wang M, Wang Z, Li X, Wang L, Wang H (2022) Ultralow-content Pd in-situ incorporation mediated hierarchical defects in corner-etched Cu_2O octahedra for enhanced electrocatalytic nitrate reduction to ammonia. Appl Catal B Environ 306:121094. https://doi.org/10.1016/j.apcatb.2022b.121094

Xu Y, Wu R, Zhang J, Shi Y, Zhang B (2013) Anion-exchange synthesis of nanoporous FeP nanosheets as electrocatalysts for hydrogen evolution reaction. Chem Commun (camb) 49(59):6656–6658. https://doi.org/10.1039/c3cc43107j

Yao Q, Chen J, Xiao S, Zhang Y, Zhou X (2021) Selective electrocatalytic reduction of nitrate to ammonia with nickel phosphide. ACS Appl Mater Interfaces 13(26):30458–30467. https://doi.org/10.1021/acsami.0c22338

Ye S, Chen Z, Zhang G, Chen W, Peng C, Yang X, Zheng L, Li Y, Ren X, Cao H, Xue D, Qiu J, Zhang Q, Liu J (2022) Elucidating the activity, mechanism and application of selective electrosynthesis of ammonia from nitrate on cobalt phosphide. Energy Environ Sci 15(2):760–770. https://doi.org/10.1039/d1ee03097c

Yin H, Chen Z, Xiong S, Chen J, Wang C, Wang R, Kuwahara Y, Luo J, Yamashita H, Peng Y, Li J (2021) Alloying effect-induced electron polarization drives nitrate electroreduction to ammonia. Chem Catal 1(5):1088–1103. https://doi.org/10.1016/j.checat.2021.08.014

Yin Z, Liu J, Jiang L, Chu J, Yang T, Kong A (2022) Semi-enclosed Cu nanoparticles with porous nitrogen-doped carbon shells for efficient and tolerant nitrate electroreduction in neutral condition. Electrochim Acta 404:139585. https://doi.org/10.1016/j.electacta.2021.139585

Yu Y, Wang C, Yu Y, Wang Y, Zhang B (2020) Promoting selective electroreduction of nitrates to ammonia over electron-deficient Co modulated by rectifying Schottky contacts. SCIENCE CHINA Chem 63(10):1469–1476. https://doi.org/10.1007/s11426-020-9795-x

Zhang H, Wang G, Wang C, Liu Y, Yang Y, Wang C, Jiang W, Fu L, Xu J (2022a) CoP nanowires on carbon cloth for electrocatalytic NOx− reduction to ammonia. J Electroanal Chem 910:116171. https://doi.org/10.1016/j.jelechem.2022.116171

Zhang X, Shen B, Shen F, Zhang X, Si M, Yuan P (2017) The behavior of the manganese-cerium loaded metal-organic framework in elemental mercury and NO removal from flue gas. Chem Eng J 326:551–560. https://doi.org/10.1016/j.cej.2017.05.128

Zhang X, Wang Y, Liu C, Yu Y, Lu S, Zhang B (2021) Recent advances in non-noble metal electrocatalysts for nitrate reduction. Chem Eng J 403:126269. https://doi.org/10.1016/j.cej.2020.126269

Zhang Y, Chen X, Wang W, Yin L, Crittenden JC (2022) Electrocatalytic nitrate reduction to ammonia on defective Au1Cu (111) single-atom alloys. Appl Catal B Environ 310:121346. https://doi.org/10.1016/j.apcatb.2022b.121346